IC FOR
AND CORRELATIVE ANALYSIS OF SIGNALS

24 JULY 1979 (FOUO) 1 OF 1

JPRS L/8586

24 July 1979

Translation

ACOUSTOOPTIC DEVICES FOR SPECTRAL AND CORRELATIVE ANALYSIS OF SIGNALS

By

S. V. Kulakov

FBIS FOREIGN BROADCAST INFORMATION SERVICE

NOTE

JPRS publications contain information primarily from foreign newspapers, periodicals and books, but also from news agency transmissions and broadcasts. Materials from foreign-language sources are translated; those from English-language sources are transcribed or reprinted, with the original phrasing and other characteristics retained.

Headlines, editorial reports, and material enclosed in brackets [] are supplied by JPRS. Processing indicators such as [Text] or [Excerpt] in the first line of each item, or following the last line of a brief, indicate how the original information was processed. Where no processing indicator is given, the information was summarized or extracted.

Unfamiliar names rendered phonetically or transliterated are enclosed in parentheses. Words or names preceded by a question mark and enclosed in parentheses were not clear in the original but have been supplied as appropriate in context. Other unattributed parenthetical notes within the body of an item originate with the source. Times within items are as given by source.

The contents of this publication in no way represent the policies, views or attitudes of the U.S. Government.

For further information on report content call (703) 351-2938 (economic); 3468 (political, sociological, military); 2726 (life sciences); 2725 (physical sciences).

APPROVED FOR RELEASE: 2007/02/09: CIA-RDP82-00850R000100070031-9

JPRS L/ 8586

24 July 1979

ACOUSTOOPTIC DEVICES FOR SPECTRAL AND CORRELATIVE ANALYSIS OF SIGNALS

Leningrad AKUSTOOPTICHESKIYE USTROYSTVA SPEKTRAL'NOGO I KORRELYATSIONNOGO ANALIZA SIGNALOV in Russian 1978 signed to press 27 Jul 78 pp 24-29, 41-55, 80-103, 138-143

[Excerpts from book by S. V. Kulakov, "Nauka" Publishing House, 144 pages, 2000 copies]

CONTENTS PAGE

PUBLICATION DATA

English title	:	ACOUSTOOPTIC DEVICES FOR SPECTRAL AND CORRELATIVE ANALYSIS OF SIGNALS
Russian title	:	AKUSTOOPTICHESKIYE USTROYSTVA SPEKTRAL'NOGO I KORRELYATSIONNOGO ANALIZA SIGNALOV
Author (s)	:	S. V. Kulakov
Editor (s)	:	
Publishing House	:	Nauka
Place of Publication	:	Leningrad
Date of Publication	:	1978
Signed to press	:	27 Jul 78
Copies	:	2000
COPYRIGHT	:	Izdatel'stvo "Nauka", 1978

UDC 621.391.14

ACOUSTOOPTIC DEVICES FOR SPECTRAL AND CORRELATIVE ANALYSIS OF SIGNALS

Leningrad AKUSTOOPTICHESKIYE USTROYSTVA SPEKTRAL'NOGO I KORRELYATSIONNOGO ANALIZA SIGNALOV in Russian 1978, Nauka pp 24-29, 41-51, 52-55, 80-103, 138-143

[Excerpts from a book by S. V. Kulakov]

1.4. The Acoustic Light Modulator [ALM] as an Element of an Optical Signal Processing System pp 24-29

When solving analysis and synthesis problems, optical information processing systems take the form of a set of individual elements with the corresponding couplings between them. The majority of the elements of an optical system (lenses, free space layers, spatial band filters, and so on) are linear with respect to the light wave transmitted through them. For these elements, in a number of papers [22, 77] both the transmitting functions and the responses to the corresponding δ-effects are defined, that is, the characteristics analogous to the characteristics of linear electric circuits are found. Such electrical analogies turn out to be highly useful when calculating optical systems, for they permit the use of the methods and mathematical apparatus well developed for analysis and synthesis of electric circuits and systems.

The devices used to input the processed information (signals) to the optical systems -- the spatial light modulators -- are also characterized by the transmission functions of the light wave incident on them. These transmission functions are sometimes called transmission coefficients, transparency functions, and so on.

For the acoustic light modulator, along with the transmission coefficients it is expedient to find the frequency-dependent coefficient which defines the linear transformation of the input electric signal to an acoustical wave packet propagated in the acoustooptic interaction medium. This coefficient will be called the electroacoustical transmission coefficient. Let us also find the electrooptical impulse response of the modulator.

Let us define the spectrum of the spatial frequencies of the acoustic wave packet corresponding to the electric signals s(t). To begin with, we shall assume that in the acoustooptic interaction medium there is no damping of the

elastic waves, and the electrooptical converter of the modulator has an infinite pass band.

The time-space signal in the aperture of the acoustic light modulator (the acoustic wave packet) corresponding to the input signal s(t) can be written in the following form:

$$f_r(z, vt) = r(z) f(vt - z), \tag{1.4.1}$$

where r(z) is the weight function defined by the aperture stop.

Let us find the Fourier transformation of the signals (1.4.1):

$$\int_{-\infty}^{+\infty} f_r(z, vt) \exp(-j\omega_z z)\, dz = \int_{-\infty}^{+\infty} r(z) f(vt - z) \exp(-j\omega_z z)\, dz. \tag{1.4.2}$$

Here $\omega_z = -\omega/v = 2\pi/\lambda_{audio}$ is the spatial frequency [30, 77], ω is the angular dynamic frequency.

Substituting the variable in (1.4.2), we obtain

$$\int_{-\infty}^{+\infty} f_r(z, vt) \exp(-j\omega_z z)\, dz = \exp(-j\omega_z vt) \int_{-\infty}^{+\infty} r(vt - y) f(y) \exp(j\omega_z y)\, dy. \tag{1.4.3}$$

The integral of type $\int_{-\infty}^{+\infty} r(vt - y) f(y) \exp(j\omega_z y) dy$ is very similar with respect to form to the integral defining the instantaneous spectrum [56]. Therefore we shall call

$$F_L^*(\omega_z, vt) = \int_{-\infty}^{+\infty} r(vt - y) f(y) \exp(j\omega_z y) dy \tag{1.4.4}$$

the instantaneous spectrum of the spatial frequencies (or the spatial instantaneous spectrum) of the mirror image of the signal f(y).

Let us rewrite expression (1.4.4) in the following form:

$$F_L^*(\omega_z, vt) = \int_{-\infty}^{+\infty} r(z) f(vt - z) \exp[j\omega_z (vt - z)]\, dz. \tag{1.4.5}$$

Taking the inverse Fourier transformation of the left and right sides of (1.4.5), we obtain

$$r(z) f(vt - z) = \frac{1}{2\pi} \int_{-\infty}^{+\infty} F_L^*(\omega_z, vt) \exp[-j\omega_z (vt - z)]\, d\omega_z. \tag{1.4.6}$$

The expression (1.4.6) defines the spatial signal in the aperture of the ALM as the set of harmonic waves of the type exp $[-j\omega_z (vt-z)]$.

Let us express the spatial instantaneous spectrum in terms of the spatial spectra of the signal and the weight function defined by the aperture stop.

Using the known theorem of the spectrum of the product of two functions [12], we have

$$F_L^*(\omega_z, vt) = \frac{1}{2\pi}\int_{-\infty}^{+\infty} F^*(\omega_z')\,\dot{R}(\omega_z - \omega_z')\exp[j(\omega_z - \omega_z')vt]\,d\omega_z', \tag{1.4.7}$$

where $F^*(\omega_z)$ is the complex-conjugate spatial spectrum of the signal, $\dot{R}(\omega_z)$ is the spatial spectrum of the weight function.

In the special case where

$$r(z) = \begin{cases} 1 \text{ for } -\frac{L}{2} \leqslant z \leqslant +\frac{L}{2}, \\ 0 \text{ for } |z| > \frac{L}{2}, \end{cases} \tag{1.4.8}$$

expression (1.4.7) assumes the form

$$F_L^*(\omega_z, vt) = \frac{1}{\pi}\int_{-\infty}^{+\infty} F^*(\omega_z')\frac{\sin(\omega_z - \omega_z')\frac{L}{2}}{\omega_z - \omega_z'} \times \exp[j(\omega_z - \omega_z')vt]\,d\omega_z', \tag{1.4.9}$$

where L is the size of the ALM aperture in the direction of propagation of the elastic waves,

Thus,

$$r(z)f(vt - z) = \frac{1}{2\pi}\int_{-\infty}^{+\infty} \exp[-j\omega_z(vt - z)]\,d\omega_z \times$$

$$\times \frac{1}{\pi}\int_{-\infty}^{+\infty} F^*(\omega_z')\frac{\sin(\omega_z - \omega_z')\frac{L}{2}}{\omega_z - \omega_z'}\exp[j(\omega_z - \omega_z')vt]\,d\omega_z'. \tag{1.4.10}$$

Expression (1.4.10) defines the time-space signal in the aperture of the ideal ALM.

Now let us take into account the distortions which are introduced by the electroacoustical (most frequently piezoelectric) converter and the damping effect of the elastic waves in the acoustooptic interaction medium of the modulator.

The piezoelectric converter can be considered as a linear quadripole with input electric signal and output electric signal, and a complex transmission coefficient $K_\pi(\omega)$ can be assigned to it. This transmission coefficient also takes into account the effect of the binding layer between the piezoconverter and a acoustooptic interaction medium, and it can be determined experimentally.

If the input signal s(t) has the spectral density $\dot{S}(\omega)$, it is obvious that

$$F^*(\omega_z) = S^*(\omega_z)\,K_\pi^*(\omega_z), \tag{1.4.11}$$

where * is the sign of complex conjugation.

The actual acoustooptic interaction medium is characterized by the damping coefficient $\alpha(\omega)$. Consequently, the time-space signal in the aperture of the ALM must be represented by the set of damping elementary waves of the type $\exp[-|\alpha(\omega_s)|z|\exp[-j\omega_s(vt-z)]$.

Thus, the actual time-space signal in the aperture of the ALM can be represented in the following form:

$$r(z)\,s(vt,\ z)=\frac{1}{2\pi}\int\limits_{-\infty}^{+\infty}\exp[-|\alpha(\omega_s)|z]\exp[-j\omega_s(vt-z)]\,d\omega_s\times$$

$$\times\frac{1}{\pi}\int\limits_{-\infty}^{+\infty}S^*(\omega_s')\,K_{\text{п}}^*(\omega_s')\frac{\sin(\omega_s-\omega_s')\frac{L}{2}}{\omega_s-\omega_s'}\exp[j(\omega_s-\omega_s')vt]\,d\omega_s'. \qquad (1.4.12)$$

The presence of damping of the elastic waves in the acoustooptic interaction medium requires the introduction of corrections to the determination of the instantaneous spectrum of the spatial frequencies.

By the instantaneous spectrum of the spatial frequencies of the time-space signal in the rectangular apperture of the ALM we mean the spectrum defined by the expression

$$F_L^*(\omega_s,\ z,\ vt)=\exp[-|\alpha(\omega_s)|z]\frac{1}{\pi}\int\limits_{-\infty}^{+\infty}S^*(\omega_s')\,K_{\text{п}}^*(\omega_s')\times$$

$$\times\frac{\sin(\omega_s-\omega_s')\frac{L}{2}}{\omega_s-\omega_s'}\exp[j(\omega_s-\omega_s')vt]\,d\omega_s'. \qquad (1.4.13)$$

Then

$$r(z)\,s(vt,\ z)=\frac{1}{2\pi}\int\limits_{-\infty}^{+\infty}F_L^*(\omega_s,\ z,\ vt)\exp[-j\omega_s(vt-z)]\,d\omega_s \qquad (1.4.14)$$

is the time-space signal in the aperture of the real ALM.

The frequency properties of the real ALM are completely defined by the product

$$K^*(\omega_s,\ z)=K_{\text{п}}^*(\omega_s)\exp[-|\alpha(\omega_s)|z], \qquad (1.4.15)$$

which we shall call the ALM electroacoustical transmission coefficient.

This coefficient establishes a unique relation between the spectrum of the input electric signal and the instantaneous spectrum of the spatial frequencies of the time-space signal in the aperture of a real acoustic light modulator.

On feeding a δ pulse to the input of the ALM at the time t, we call the time-space signal in the aperture of the ALM the electroacoustical impulse response. Substituting the spectral density $\dot{S}(\omega) = \exp(-j\omega\tau)$ in (1,4,12), for the electroacoustical impulse response of the ALM we obtain

$$g(vt,\ v\tau,\ z) = \frac{1}{2\pi}\int_{-\infty}^{+\infty} \exp[-|\alpha(\omega_s)|z] \times$$

$$\times \exp[-j\omega_s(vt - z)]\, d\omega_s \frac{1}{\pi}\int_{-\infty}^{+\infty} \exp(j\omega'_s v\tau)\, K_{\text{п}}^{*}(\omega'_s) \times$$

$$\times \frac{\sin(\omega_s - \omega'_s)\frac{L}{2}}{\omega_s - \omega'_s} \exp[j(\omega_s - \omega'_s)vt]\, d\omega'_s. \qquad (1.4.16)$$

Then the time-space signal in the aperture of the acoustic light modulator with aperture input signal can be found using the known expression

$$r(z)\, s(vt,\ z) = \int_{-\infty}^{+\infty} s(v\tau)\, g(vt,\ v\tau,\ z)\, dv\tau. \qquad (1.4.17)$$

It must be noted that the electroacoustical transmission coefficient and the impulse response of the SLM are not related to each other by the Fourier transformation. However, these characteristics completely reflect the frequency and time characteristics of the linear process of conversion of the input electric signal to the time-space signal in the ALM aperture.

As was indicated in item 1.1, various operating conditions of the diffraction acoustic light modulator are distinguished. The modulation process is most simply described under Raman-Nutt conditions when purely phase modulation is assumed. We shall limit ourselves to the investigation of this case here.

Let the electric signal s(t) be fed to the input of the acoustic light modulator operating under the Raman-Nutt conditions. The plane light wave incident normally on the ALM

$$e'(t,\ x) = E_0 \exp[j(\omega_{\text{св}}t - k_{\text{св}}x)]$$
(1)

Key: 1, light

is modulated by the time-space signal, and at the output of the modulator it can be represented by the expression

$$e'(t,\ vt) = E_0 \exp j[\omega_{\text{св}}t + Ar(z)\, s(vt,\ z)], \qquad (1.4.18)$$

where A is the proportionality coefficient. With a harmonic input signal it has the meaning of the phase modulation index (the phase advance $k_{\text{light}}x$ which is insignificant to the following discussion will be omitted just as in item 1.3.) Thus, the ALM operating in the Raman-Nutt diffraction mode has the following transmission coefficient of the light wave incident on it:

$$T(vt, z) = \exp[jAr(z)s(vt, z)]. \qquad (1.4.19)$$

Here the exponent in (1.4.19) is determined by the diffraction activity of the acoustooptic interaction medium and the expressions (1.4.14) or (1.4.17) establishing the relation between the input electric signal s(t) and the time-space signal in the aperture of the ALM.

The acoustic light modulator is a linear device with respect to the light wave normally incident on it. At the same time the nonlinear transformation of the input electric signal of the type (1.4.19) satisfies the generalized superposition principle [11]. This fact can be used both for analysis and synthesis of the acoustooptic devices and, obviously, for the solution of the problem of linearization of their amplitude characteristics.

2.2. Multichannel Acoustooptic Spectral Devices pp 41-51

In radio engineering the problem frequently arises of analyzing a multidimensional signal made up of N elementary independent electric signals existing in separate channels or separated in space. As a rule, these elementary signals are distinguished by initial phases. Specialized optical computers to which the elementary signals are input by means of multichannel ALM find application in the processing of multidimensional signals [3, 83, 97, 104, 121]. Sometimes these devices are not so precisely called multichannel acoustooptic spectral analyzers, although the term "multichannel analyzer" presupposes the presence of N independent channels and, consequently, N output (in the general case, two dimensional) signals. In the investigated device N elementary input signals (or one N-dimensional input signal) forms one output (in the general case, three dimensional) signal. Inasmuch as the operating principle of this acoustooptic computer consists in formation of the light wave spectrum modulated by the signals in the multichannel ALM, we shall call it a multichannel acoustooptic spectral device.

The most prospective is the application of the multichannel acoustooptic spectral devices for processing multidimensional electric signals of phased antenna arrays.

In 1963, a multichannel acoustooptic device was described in reference [83] for simultaneous observation of many radar targets. In this device the signals from the elements of the linear antenna array were fed after frequency conversion and amplification to piezoquartz electroacoustic converters attached to one end of an acoustic polygon (a multichannel acoustic light modulator). Here the phases of the signals transmitted to the polygon repeated the phases of the signals reaching the elements of the antenna array. The distances between the electroacoustic converters on the scale determined by the ratio of the lengths of the electromagnetic and elastic waves corresponded to the distances between elements of the antenna array. Thus, the total elastic wave created by the linear acoustic array was propagated in the acoustic polygon at the angle to the acoustic array at which the electromagnetic wave was incident on the antenna array.

The acoustic polygon was illuminated by collimated light, and in the rear focal plane of the integrating objective, series were formed, each pair of which (with small phase modulation indexes) corresponded to the radar target observed at the corresponding angle. By measuring the angular position of the diffraction spot, it was possible to determine the angular coordinate of the radar target. In spite of the quite similar description of a device presented in the indicated paper, it did not become widespread as a result of technical difficulties connected with execution of it.

In reference [97] a study was made of the application of the acoustooptic spectral devices for processing the signals of a phased antenna array (PAA). Two methods of processing the signals of the linear receiving antenna array are described: 1) multiple time delay and 2) spatial multichannel nature. The combination of these methods makes it possible to create a device for processing the signals of a planar PAA. Let us discuss them in more detail.

The functional diagram of the signal processing device of the linear PAA which uses the multiple time delay method is presented in Figure 13. The pulse signals induced in the elements of the linear PAA reach the frequency converters; then they are delayed by the corresponding time and summed. The magnitudes of the time delay are selected so that the total signal will consist of N radial pulses (where N is the number of elements of the PAA), the interval between which would be proportional to the angle of incidence ϕ of a plane electromagnetic wave incident on the PAA. The total signal is fed to a single-channel acoustooptic spectral analyzer. The position of the main lobe of the diffraction peak of the first order is determined by the average frequency of the total pulse and, consequently, depends on the angle ϕ.

The functional diagram of the acoustooptic signal processing device of the linear PAA executed by the method of spatial multichannelness is presented in Figure 14. The signals from the elements of the PAA are fed after frequency conversion and amplification to the corresponding electroacoustic converters of the multichannel ALM, which is illuminated by a plane monochromatic light wave I. A diffraction pattern is formed in the rear focal plane of the integrating objective. Here the position of the main peak of the first-order diffraction maximum reckoned along the ω_y axis is defined by the angle θ at which the plane electromagnetic wave is incident on the linear PAA. By measuring the coordinate ω_y, the angle θ is determined.

If the planar PAA has N columns and M rows, then an N-channel light modulator is used in the signal processing device of such an array, and a bunch of N-pulses is created in each channel by the multiple time delay method. By measuring the coordinates ω_y and ω_z of the main peak of the first-order diffraction maximum, the angular coordinates of the observed target are determined.

In reference [97] the results are presented from experimental studies of an acoustooptic device with multichannel ALM with the following parameters:

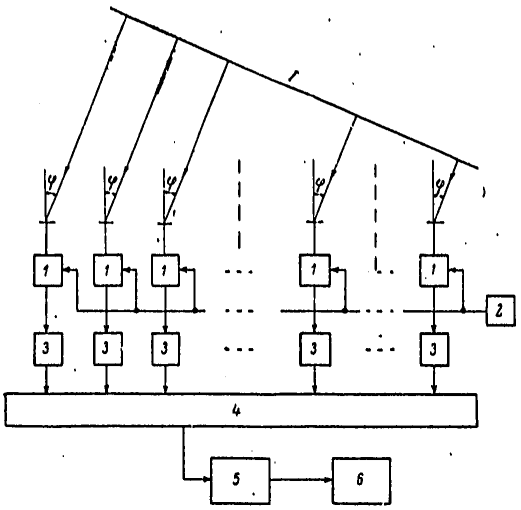

Figure 13. Functional diagram of the PAA signal processing device using the method of multiple time delay. 1 -- mixer, 2 -- heterodyne, 3 -- delay line, 4 -- adder, 5 -- spectral analyzer, 6 -- display, I -- plane electromagnetic wave front.

average pass band frequency of the channel 20 megahertz, duration of the processed signal in each channel 25 microseconds, width of the channel pass band 5 megahertz, number of channels 24.

The multichannel ALM is executed in the form of a glass cell filled with distilled water with an array of electroacoustic converters made from an x-cut piezoquartz plate on which gold electrodes are applied. The electrode width is 1.5 mm, the spacing between adjacent electrodes, 3 mm. A 4 megawatt helium-neo. laser was used as the light source. The optical system was made of high-quality optical parts. The read-outs system is a photomultiplier with narrow slits (1 micron) in front of a photocathode fastened to a moving platform. The signals from the photomultiplier were amplified by a logarithmic amplifier and fed to an automatic recorder. The experiments were performed with specially developed PAA signal simulator. The angles of incidence of a plane electromagnetic wave on a linear PAA amounting to zero and 19.5° were simulated. For these angles the distribution curves of the light intensity in the region of the first diffraction maximum were calculated. Then the actual light distribution was measured using the read-out system. The results of the measurements agree well with the calculation. The possibility of suppressing the side lobes by the weighted processing method was also checked out.

In [104, 121] it was proposed that a multichannel acoustooptic device be used to process the radio telescope signals, in particular, the signals of

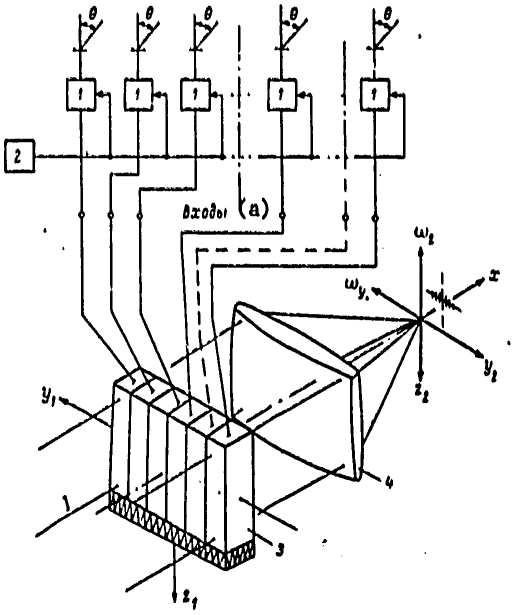

Figure 14. Functional diagram of the signal processing device of the PAA by the method of spatial multichannelness, 1 -- mixer, 2 -- heterodyne, 3 -- multichannel ALM, 4 -- integrating objective,

Key: a, inputs

a radioheliograph. An original optical system was developed. Obviously this is the most prospective application of such devices.

In the papers devoted to multichannel acoustooptic spectral devices, as a rule, studies are made of the factors determining the distribution of the light oscillations in the output plane of the optical computer for the simplest input signals. However, the procedure for calculating the output signals for arbitrary input signals is left out of these papers. Inasmuch as the investigated device belongs to the linear spectral devices, it is expedient to determine its instrument function which in the given case will be multidimensional. When determining the instrument function we use the known principles of the theory of linear multidimensional systems [13].

The superposition integral for systems with N inputs and M outputs is written as follows:

$$f(y) = \int_{y_0}^{y} G(y, x) \cdot s(x)\, dx, \qquad (2.2.1)$$

where s(x) and $\xi(y)$ are the input and output vectors of the system, G(y, x) is the pulse matrix,

If a single pulse $\delta(y - x)$ is fed to the ith input of the system, the output vector of the system has the form

$$g_i(y, x) = \begin{bmatrix} g_{1i}(y, x) \\ g_{2i}(y, x) \\ \cdots \\ g_{Mi}(y, x) \end{bmatrix}, \qquad (2.2.2)$$

where $g_{ji}(y, x)$ is the pulse response of the jth output excited by a single pulse at the ith input. Feeding the δ-effect to the remaining inputs, we determine the pulse matrix of the system

$$G(y, x) = \begin{bmatrix} g_{11}(y, x) & g_{12}(y, x) \cdots g_{1N}(y, x) \\ g_{21}(y, x) & g_{22}(y, x) \cdots g_{2N}(y, x) \\ \cdots & \cdots \\ g_{M1}(y, x) & g_{M2}(y, x) \cdots g_{MN}(y, x) \end{bmatrix}. \qquad (2.2.3)$$

for a system with N inputs and one output the pulse matrix is a row-matrix

$$G(y, x) = [g_{11}(y, x)\, g_{12}(y, x) \ldots g_{1N}(y, x)], \qquad (2.2.4)$$

and here

$$g_i(y, x) = g_{1i}(y, x). \qquad (2.2.5)$$

Let us define the pulse matrix of a multichannel acoustooptic device, the functional diagram of which is presented in Figure 14 on feeding δ-inputs in the frequency region to its inputs. This pulse matrix, by analogy with the instrument functions of the single-channel spectral devices, will be called the instrument matrix of the multichannel acoustooptic spectral device. Here it is necessary to feed a harmonic oscillation to the inputs of the spectral device

$$s_{ai}(t) = \cos \omega_{ai} t; \qquad (2.2.6)$$
(1) (2)

Key: 1. input 2. audio

Thus, the input signal in the frequency region can be written in the form

$$s_{ai}(\omega) = [\pi\delta(\omega + \omega_{ai}) + \pi\delta(\omega - \omega_{ai})]\,\xi_i \quad \text{for} \quad 1 \leqslant i \leqslant N, \qquad (2.2.7)$$

where ξ_i is the ith column of the unit matrix N × N, that is,

$$\xi_i = \begin{bmatrix} 0 \\ \vdots \\ 0 \\ 1 \\ 0 \\ \vdots \\ 0 \end{bmatrix} \rightarrow \text{ith row.} \qquad (2.2.8)$$

The plane light wave I incident on the multichannel ALM (see Figure 14) is phase-modulated by harmonic elastic waves.

In the case of identical channels of the ALM, the light wave at its output can be described as follows:

$$e'(t, z_1, y_1) = \begin{cases} E_0 \cos[\omega_{es}t - A\cos(\omega_{ss}t - k_{ss}z_1)] \cdot \xi_i & \text{for} \\ -[0.5N-(i-1)]a - [0.5(N+1)-i]b \leqslant \\ \leqslant y_1 \leqslant -(0.5N-i)a - [-0.5(N+1)-i]b, \\ 0 \text{ for } -(0.5N-i)a - [0.5(N+1)-i]b < \\ < y_1 < -(0.5N-i)a - [0.5(N+1)- \\ -(i-1)]b, \quad 1 \leqslant i \leqslant N, \end{cases} \qquad (2.2.9)$$

where a is the width of one channel of the ALM, a + b is the spacing between adjacent channels.

The analytical signal which can be represented by the following expression corresponds to the narrow-band signal (2.2.9) ($\omega_{light} >> \omega_{audio}$, $A << 1$):

$$e'(t, z_1, y_1) = \begin{cases} E_0 \exp j\omega_{es}t \sum_{m=-\infty}^{\infty} J_m(A) \exp\left[jm(\omega_{ss}t - k_{ss}z + \frac{3\pi}{2}\right]\xi_i \\ \text{for} -[0.5N-(i-1)]a - [0.5(N+1)-i]b \leqslant \\ \leqslant y_1 \leqslant -0.5(N-i)a - [0.5(N+1)-i]b, \\ 0 \text{ for } -(0.5N-i)a - [0.5(N+1)-i]b < y_1 < \\ < -(0.5N-i)a - [0.5(N+1)-(i-1)]b, \\ 1 \leqslant i \leqslant N. \end{cases} \qquad (2.2.10)$$

The analytical signal corresponding to the distribution of the light oscillations in the rear focal plane of the integrating objective is described in the form [77]

$$e'(t, \omega_z, \omega_y) = B_1 \int_{-0.5Na-0.3(N-1)b}^{0.5Na+0.3(N+1)b} \int_{-0.5L}^{+0.5L} e'(t, z_1, y_1) \times \\ \times \exp[-j(\omega_y y_1 + \omega_z z_1)]\, dy_1 dz_1, \qquad (2.2.11)$$

where

$$\omega_y = -\frac{k_{es}}{F} y_3.$$

The plus first-order diffraction maximum (the region of the output plane of the device of interest to us) is formed by the light waves defined by the terms of expression (2,2,10) for which m = 1. This region of the output plane can be considered as the only output of our spectral device with N inputs.

Limiting ourselves to the investigation of the plus first-order diffraction region, we exclude the negative spatial frequencies from the investigation.

Consequently, it is possible to talk about the spectrum of the analytical signal corresponding to the light wave modulated by an N-dimensional input signal.

Thus,

$$e'_{+1}(t,\ \omega_z,\ \omega_y) = \int\limits_{-0.5Na-0.5(N-1)b}^{+0.5Na+0.5(N+1)b}\ \int\limits_{-0.5L}^{+0.5L} e'_{+1}(t,\ z_1,\ y_1)\exp\left[-j(\omega_y y_1 + \omega_z z_1)\right] dy_1 dz_1, \tag{2.2,12}$$

where $e'_{+1}(t, \omega_z, \omega_y)$ is the analytical signal corresponding to the light oscillations in the region of the plus first-order diffraction maximum. Here

$$e'_{+1}(t,\ z_1,\ y_1) = \begin{cases} E_0 \exp(j\omega_{c_2} t)\, J_1(A) \exp\left[j\left(\omega_{s_2} t - k_{s_2} z_1 + \frac{3\pi}{2}\right)\right] \cdot \xi_i \\ \text{for} -[0.5N-(i-1)]a-[0.5(N+1)-i]b \leqslant \\ \leqslant y_1 \leqslant -0.5(N-i)a-[0.5(N+1)-i]b, \\ 0 \text{ for } -0.5(N-i)a-[0.5(N+1)-i]b < \\ < y_1 < -(0.5N-i)a-[0.5(N+1)-(i-1)]b, \\ 1 \leqslant i \leqslant N. \end{cases} \tag{2.2,13}$$

Let us consider the investigation of the ith term of expression (2.2.13):

$$e'_{+1i}(t,\ \omega_z,\ \omega_y) = B_1 E_0 J_1(A) \exp\left[j(\omega_{c_2} + \omega_{s_2})t\right] \times \int\limits_{-[0.5N-(i-1)]a-[0.5(N+1)-i]b}^{-[0.5N-(i-1)]a-[0.5(N+1)-i]b}\ \int\limits_{-0.5L}^{+0.5L} \exp\left[-j(\omega_z + k_{s_2})z_1\right] dz_1. \tag{2.2,14}$$

After simple transformations (2.2.14) is written in the following form:

$$e'_{1i}(t,\ \omega_z,\ \omega_y) = B_2 J_1(A)\, \frac{\sin 0.5(v\omega_z + \omega_{s_2})T}{0.5(v\omega_z + \omega_{s_2})T} \exp\left(j\left[(v\omega_z + \omega_{s_2})t\right]\right) \times$$
$$\times \frac{\sin 0.5a\omega_y}{0.5a\omega_y} \exp\left(j\left[0.5(N+1) - i\right](a+b)\omega_y\right]\right) \exp\left[j(\omega_{s_2} - v\omega_z)t\right], \tag{2.2,15}$$

where $B_2 = B_1 E_0 aL$, $T = L/v$.

Expression (2,2,15) defines the output signal of the device on feeding a δ-input in the frequency region to its input, that is, in essence, one element of its instrument matrix. However, as one element of the instrument row-matrix of the multichannel acoustooptic spectral device we take the cofactor

$$g_i(\omega-\omega_{ss},\ \omega_y,\ t)=\frac{\sin 0.5(\omega-\omega_{ss})T}{0.5(\omega-\omega_{ss})T}\cdot\frac{\sin 0.5a\omega_y}{0.5a\omega_y}\times$$
$$\times\exp[-j(\omega-\omega_{ss})t]\exp(j[0.5(N+1)-i](a+b)\omega_y), \qquad (2.2.16)$$

(where $\omega = -v\omega_z$) which determines the spectral distribution for A << 1, that is, for $J_1(A) \approx A/2$. The condition of smallness of the phase modulation index (that is, the input signal levels) is a necessary condition of linearity of the investigated spectral device. Thus, the latter has the instrument matrix

$$G(\omega-\omega_{ss},\ \omega_y,\ t)=[g_1(\omega-\omega_{ss},\ \omega_y,\ t)\,g_2(\omega-\omega_{ss},\ \omega_y,\ t)\dots$$
$$\dots g_N(\omega-\omega_{ss},\ \omega_y,\ t)], \qquad (2.2.17)$$

which is formed on the light carrier.

If a multidimensional signal is fed to the input of the device, and the analytical signal corresponding to it has the spectrum

$$Z_{sx}(\omega)=\begin{cases}\begin{bmatrix}Z_1(\omega)\\ Z_2(\omega)\\ \dots\\ Z_N(\omega)\end{bmatrix} & \text{for } \omega\geqslant 0,\\ 0 & \text{for } \omega<0,\end{cases} \qquad (2.2.18)$$

the output spectral distribution is written as follows:

$$Z_{sux}(\omega,\ \omega_y,\ t)=\begin{cases}\int\limits_{\omega_0-\Delta\omega_0}^{\omega_0+\Delta\omega_0} G(\omega-\omega_{ss},\ \omega_y,\ t)\,Z_{sx}(\omega_{ss})\,d\omega_{ss} & \text{for } \omega\geqslant 0,\\ 0 & \text{for } \omega<0,\end{cases} \qquad (2,2.19)$$

where ω_0 and $2\Delta\omega$ are the average frequency and the pass band width of one ALM channel. (If the ALM channels have different parameters, including average frequencies and pass bands, the integration limits will be different for the different elements of the instrument matrix).

Let us rewrite expression (2.2.19) as follows:

$$Z_{sux}(\omega,\ \omega_y,\ t)=\int\limits_{\omega_0-\Delta\omega_0}^{\omega_0+\Delta\omega_0} g_1(\omega-\omega_{ss},\ \omega_y,\ t)\,Z_1(\omega_{ss})\,d\omega_{ss}+$$
$$+\int\limits_{\omega_0-\Delta\omega_0}^{\omega_0+\Delta\omega_0} g_2(\omega-\omega_{ss},\ \omega_y,\ t)\,Z_2(\omega_{ss})\,d\omega_{ss}+\dots+ \qquad (2,2,20)$$

$$+\int_{\omega_0-\Delta\omega_0}^{\omega_0+\Delta\omega_0} g_N(\omega-\omega_{ss}, \omega_y, t)\,\dot{Z}_N(\omega_{ss})\,d\omega_{ss} \qquad \omega \geqslant 0,$$

$$\dot{Z}_{\text{(1) вых}}(\omega, \omega_y, t) = 0 \quad \text{for} \quad \omega < 0,$$

Key: 1. out 2. audio

and let us consider the integration of the common term

$$\dot{Z}_{\text{(1) вых}\,i}(\omega, \omega_y, t) = \int_{\omega_0-\Delta\omega_0}^{\omega_0+\Delta\omega_0} g_i(\omega-\omega_{ss}, \omega_y, t)\,\dot{Z}_i(\omega_{ss})\,d\omega_{ss} =$$

$$= \frac{\sin 0.5a\omega_y}{0.5a\omega_y} \exp\{j[0.5(N+1)-i](a+b)\omega_y\} \times$$

$$\times \int_{\omega_0-\Delta\omega_0}^{\omega_0+\Delta\omega_0} \frac{\sin 0.5(\omega-\omega_{ss})T}{0.5(\omega-\omega_{ss})T}\,\dot{Z}_i(\omega_{ss}) \exp[-j(\omega-\omega_{ss})]\,d\omega_{ss} \quad \text{for} \quad \omega \geqslant 0, \qquad (2.2.21)$$

Key: 1. out

As is demonstrated in item 2.1, the integral in expression (2.2.21) defines the instantaneous spectrum of the analytical signal corresponding to the signal $s_i(t)$ at the ith input of the device.

Thus,

$$\dot{Z}_{\text{(1) вых}\,i}(\omega, \omega_y, t) =$$

$$= \begin{cases} \dfrac{\sin 0.5a\omega_y}{0.5a\omega_y} \exp\{j[0.5(N+1)-i](a+b)\omega_y\}\,\dot{Z}_{iT}(\omega, t) & \text{for } \omega \geqslant 0, \\ 0 & \text{for } \omega < 0. \end{cases} \qquad (2.2.22)$$

Key: 1. out

The signal corresponding to the spectral distribution (2.2.22) is formed on the carrier $e_{1i}(t, \omega) = \exp[j(\omega_{light} - \omega)t]$.

Considering (2.2.22), (2.2.20), will be rewritten in the following form:

$$\dot{Z}_{\text{вых}}(\omega, \omega_y, t) = \begin{cases} \dfrac{\sin 0.5a\omega_y}{0.5a\omega_y} \exp\{j0.5(N+1)(a+b)\omega_y\} \sum_{i=1}^{N} \dot{Z}_{iT}(\omega, t) \times \\ \times \exp[-j0.5i(a+b)\omega_y] \quad \text{for} \quad \omega \geqslant 0, \\ 0 \quad \text{for} \quad \omega < 0. \end{cases} \qquad (2.2.23)$$

Using the expressions obtained, let us calculate the distribution of the light oscillations in the output plane of the multichannel acoustooptic spectral device as applied to the problem of processing the signals of a linear phased antenna array.

Let us propose that a plane electromagnetic wave is incident on the antenna array at an angle θ. The signals induced in the antenna elements are amplified, they are frequency converted and reach the corresponding inputs of the multichannel acoustooptic spectral device. Let us also propose that the signals in the channels have identical levels, and the channels themselves are identical. Then the spectral densities of the signals will differ only by the phase factors $\exp(-j\Delta\phi_i)$, where $\Delta\phi_i = (i-1)\omega_{em}(d/v_{light})\sin\theta$ is the phase difference between the signals of the first and the ith channels, and ω_{em} is the frequency of the electromagnetic oscillations incindent on the antenna array, d is the spacing between adjacent elements of the antenna array. Here

$$Z_{вых}(\omega, \omega_y, t) = \begin{cases} \frac{\sin 0.5a\omega_y}{0.5a\omega_y} \exp\{j0.5(N+1)(a+b)\omega_y\} \dot{Z}_T(\omega, t) \times \\ \times \sum_{i=1}^{N} \exp\{-j(i-1)\Delta\varphi\} \exp\{-j0.5i(a+b)\omega_y\} \\ \qquad \text{for } \omega \geqslant 0, \\ 0 \qquad \text{for } \omega < 0. \end{cases} \quad (2.2.24)$$

(1)

Key: 1. out

Then the analytical signal corresponding to the distribution of the light oscillations in the region of formation of the plus first-order diffraction maximum will be defined by the expression

$$\dot{e}'_{+1}(\omega, t, \omega_y) = B_3 \frac{A}{2} \frac{\sin 0.5a\omega_y}{0.5a\omega_y} \cdot \frac{\sin 0.5N\left[(a+b)\omega_y + \omega_{вх}\frac{d}{v_{св}}\sin\theta\right]}{\sin 0.5\left[(a+b)\omega_y + \omega_{вх}\frac{d}{v_{св}}\sin\theta\right]} \times$$
$$\times \exp\left(-j\frac{N-1}{2}\omega_{вх}\frac{d}{c}\sin\theta\right) 2\dot{S}_T(\omega, t)\exp\{j(\omega_{св}-\omega)t\}, \quad (2.2.25)$$

where $\dot{S}_T(\omega, t)$ is the instantaneous signal spectrum in the first channel of the ALM.

The expression (2.2.25) indicates that the distribution of the light oscillations with respect to the ω_y axis has a multilobe nature. Here the position of the main peak can be found from the expression

$$\omega'_y = \frac{\omega_{вх}\frac{d}{v_{св}}\sin\theta}{a+b}. \quad (2.2.26)$$

The spacing reckoned from the point corresponding to $\theta = 0$ to the point corresponding to the nonzero value of θ in the rear focal plane of the integrating objective for $d = \lambda_{em}/2$ (where $\lambda_{em} = 2\pi v_{light}/\omega_{em}$) is equal to

$$y'_2 = \frac{\lambda_{св}F}{2(a+b)}\sin\theta. \quad (2.2.27)$$

The width of the main maximum $2\Delta y_2$ of the function (2.2.25) with respect to the zero values for $d = \lambda_{em}/2$ can be found from the expression

$$2\Delta y_2 = \frac{2\lambda_{ak} F}{(a+b)N}. \qquad (2.2.28)$$

On variation of the angle θ, a shift in the position of the main maximum of the function (2.2.25) takes place. By measuring this shift it is possible to find the anglular coordinate of the target θ:

$$\theta = \arcsin \frac{2(a+b)y_2'}{\lambda_{ak} F}. \qquad (2.2.29)$$

Expression (2.2.25) also indicates that the distribution of the light oscillations with respect to the ω_z axis will be defined by the instantaneous spectrum of the input signal. This coordinate can be used on application of the multiple time delay method which combined with the method of spatial multitime channelness will permit processing of the signals of the planar antenna arrays [97].

Chapter 3. CORRELATIVE ACOUSTOOPTIC SIGNAL pp 52-55

The correlative acoustooptic signal analysis devices are of great interest at the present time. This is explained by the high potential possibilities. In spite of the fact that these possibilities have not been fully realized as yet as a result of the great technical difficulties, the acoustooptic devices forming the convolution of input signals (convolvers) or their correlation functions (correlators) are finding different applications in modern radio electronics.

The basic reason why attention has been turned to the acoustooptic correlative analysis devices is the possibility of building instruments which operate in real time.

The ALM available at the present time permit the creation of devices which can be used both in the intermediate radio frequency range (to 100 megahertz) and in the high and superhigh frequency bands. This greatly expands the region of application of the acoustooptic correlative analysis devices and makes it possible to use them to solve a variety of problems.

The devices built on the basis of the acoustooptic correlators and convolvers -- parametric quadripoles, time scale converters and dispersion spectral analyzers -- also have great practical significance.

When investigating such devices we shall first discuss some of the publications on acoustooptic convolvers and correlators and then proceed with their analysis and various applications.

3.1. Acoustooptic Convolvers and Correlators

The functional diagram of the simplest acoustooptic convolver [63, 92, 111] is presented in Figure 15. The device includes a light source 1, the condenser 2, the collimator 3, the ALM I 4, the ALM II 5, the integrating objective 6 and the photodetectors 7 (photomultiplier) with electric band filter as the load.

The light source, the condenser and collimator create a plane light wave which illuminates the first acoustic light modulator 4. In the ALM I an elastic wave packet is propagated which corresponds to the electric signal which reached the electroacoustic converter (input I). On passage through the ALM I the plane light wave is phase-modulated and then illuminates the second acoustic light modulator 5. The second of the signals is fed to the input II, that is, to the ALM II. The elastic wave packet corresponding to the signal secondarily modulates the light wave. (A traveling wave regime is created in the modulators as a result of using acoustic absorbers).

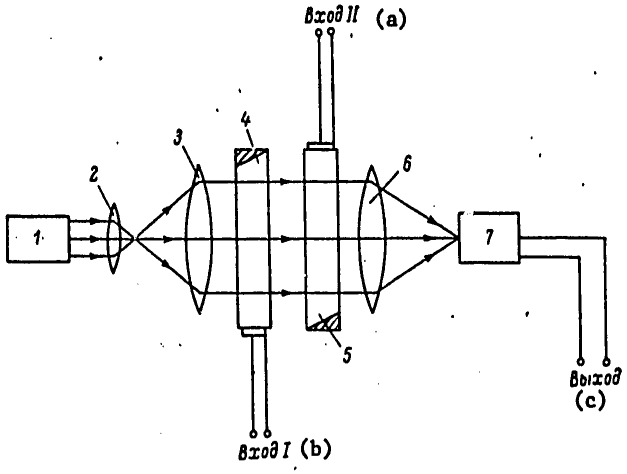

Figure 15. Functional diagram of the simplest acoustooptic convolver.

Key: a. input II b. input I c. output

The successive passage of the light through two modulators provides for multiplication of the time-space signals corresponding to the input electric signals. The counter propagation of elastic wave packets insures the signal shift required for shaping the convolution and the mirror image of one of the time-space signals with respect to the selected positive direction of the spatial coordinate.

The integrating objective which gathers light from all parts of the aperture, provides for the execution of the integration operations. The photodetector converts the modulated light flux to an electric signal corresponding to convolution of the input signal of the device.

When using the acoustooptic convolver for purposes of correlative analysis of signals, it must be supplemented by the time scale converter for one of the signals, which shapes the inverse time scale.

The electroacoustic device for forming the inverse time scale (the device for forming the mirror image of the signal in time) is described in reference [111] (see Figure 16). It contains a light source 1, a collimator 2, projection objectives 5-7, integrating objectives 10, ALM I 12, ALM II 8, polarizer 3, analyzers 4, 9, a quarter-wave plate 13 and photodetector 11. The processed signal is fed to the input of the device, that is, to the ALM I. The ALM I is illuminated by the light with circular polarization created by the polarizer and the quarter-wave plate ("optical shift"). The image of the processed signal is shaped by the projection objectives on the ALM II with twofold diminishing. A delta pulse is fed to the input of the ALM II with a delay equal to the duration of the processed signal. The elastic wave packet corresponding to this delta pulse and the image of the processed signal are shifted in the same direction, but with different velocities.

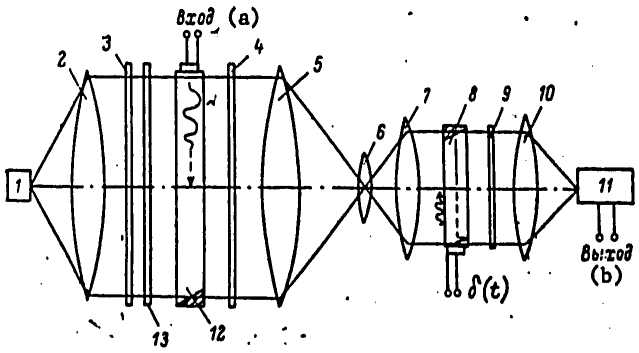

Figure 16. Acoustooptic device for shaping the mirror image in time of the processed signal.

Key: a. output b. input

Here, the elastic wave packet corresponding to the delta pulse overtakes the image of the processed signal and reads it from the end. The integrating objective which gathers light from the entire apperture of the device executes the integration operation, and the photodetector (photomultiplier) converts the time-modulated light flux to an electric signal, which is the

mirror image in time of the input signal. In essence, shaping of the mutual-correlation function of the input signal and the delta pulse occurs here. An analogous device executed on the basis of diffraction ALM is proposed by the author of [33].

An original small-scale optical system of an acoustooptic convolver is described in [89]. The device has high structural parameters, for the same optical elements are used many times, and various functions are performed.

In reference [63] the oscillograms of the output signals are presented for the processing of signals with intrapulse phase manipulation by the simplest convolver in accordance with the five-valued and 13-valued Barker codes on a carrier frequency of 15 megahertz.

In [81, 82] the possibility of processing the signals with the product of the duration times the spectral width of 10^3 to 10^4 by acoustooptic convolvers is indicated. For example, there is a description here of an original small-scale device with ALM of complex form. The possibility of processing signals lasting 340 microseconds on a carrier frequency of 30 megahertz is indicated. The oscillograms of the output signals are presented for feeding signals with phase manipulation to the input.

Connecting a device for shaping the mirror image of the signal in time to one of the inputs of the convolver, we obtained the possibility of correlation analysis of the signals. Such a correlator, which contains acoustooptic convolver and device for shaping a mirror image is described in [111].

3.5. Dispersion Quadripoles Based on an Acoustooptic Device with Enlarged Image of the Reference LFM [Linear Frequency-Modulated] Signal pp 80-103

Let the quadripole reference signal generator, the functional diagram of which is illustrated in Figure 19, shape the LFM signal

$$s_{0\pi}(t-T_3)=\cos\left[\omega_{0\pi}\left(t-\frac{T_{0\pi}}{2}-T_3\right)-\frac{\beta_{0\pi}}{2}\left(t-\frac{T_{0\pi}}{2}-T_3\right)^2\right], \qquad (3.5.1)$$

(1)

Key: 1. reference

where $\beta_{ref} = 2\omega_{d.ref}/T_{ref}$, $\omega_{d.ref}$ is the frequency deviation in the reference signal.

If all of the diffraction peaks of the plane of spatial frequencies are used to construct the image of the reference signal (for small phase modulation indexes, the zero and first order diffraction peaks are used), then considering (3.2.17) and (3.3.1) we write (3.5.1) for Q = -1 in the following form:

$$\underline{s}_{on}(t-T_s)=\cos\left[\omega_0 P\left(t-\frac{T_{on}}{2}-T_s\right)-\frac{\beta_0 P^2}{2}\left(t-\frac{T_{on}}{2}-T_s\right)^2\right], \qquad (3.5.2)$$

where $\beta_0 = 2\Delta\omega_0/PT_{ref}$, $2\Delta\omega_0$ is the pass band of the ALM II.

Considering (3.3.8) and (3.3.9) for $T_{ref} < T_{inp}/P$ let us write the pulse response of the quadripole in terms of the set of normal pulse responses

$$g(\xi,\tau)=\begin{cases} B\cos\left[\omega_0\left(\xi-\tau_i-\frac{PT_{on}}{2}\right)-\frac{\beta_{on}}{3}\left(\xi-\tau_i-\frac{PT_{on}}{2}\right)^2\right] \\ \text{for } -T_{on}\leqslant\tau_i\leqslant 0 \text{ for } \tau_i\leqslant\xi\leqslant(P+1)\tau_i+PT_{on}, \\ B\cos\left[\omega_0\left(\xi-\tau_i-\frac{PT_{on}}{2}\right)-\frac{\beta_{on}}{2}\left(\xi-\tau_i-\frac{PT_{on}}{2}\right)^2\right] \\ \text{for } 0<\tau_i\leqslant T_{ax} \text{ for } \tau_i\leqslant\xi\leqslant\tau_i+PT_{on}, \\ B\cos\left[\omega_0\left(\xi-\tau_i-\frac{PT_{on}}{2}\right)-\frac{\beta_{on}}{3}\left(\xi-\tau_i-\frac{PT_{on}}{2}\right)^2\right] \\ \text{for } T_{ax}<\tau_i\leqslant T_{on}+T_{ax} \text{ for } (P+1)\tau_i-PT_{ax}\leqslant\xi\leqslant\tau_i+PT_{on}, \end{cases} \qquad (3.5.3)$$

Key: 1. op = reference

and the set of conjugate pulse responses

$$g(\tau,\xi)=\begin{cases} B\cos\left[\omega_0\left(\tau-\xi_i+\frac{PT_{on}}{2}\right)+\frac{\beta_{on}}{2}\left(\tau-\xi_i+\frac{PT_{on}}{2}\right)^2\right] \\ \text{for } -T_{on}\leqslant\xi_i\leqslant PT_{on} \text{ for} \frac{\xi_i-PT_{on}}{P+1}\leqslant\tau\leqslant\xi_i, \\ B\cos\left[\omega_0\left(\tau-\xi_i+\frac{PT_{on}}{2}\right)+\frac{\beta_{on}}{2}\left(\tau-\xi_i+\frac{PT_{on}}{2}\right)^2\right] \\ \text{for } PT_{on}<\xi_i\leqslant T_{ax} \text{ for } \xi_i-PT_{on}\leqslant\tau\leqslant\xi_i, \\ B\cos\left[\omega_0\left(\tau-\xi_i+\frac{PT_{on}}{2}\right)-\frac{\beta_{on}}{2}\left(\tau-\xi_i+\frac{PT_{on}}{2}\right)^2\right] \\ \text{for } T_{ax}<\xi_i\leqslant(P+1)T_{on}+T_{ax} \text{ for } \xi_i-PT_{on}\leqslant\tau\leqslant\frac{\xi+PT_{ax}}{P+1}. \end{cases} \qquad (3.5.4)$$

(1) (2)

Key: 1. reference 2. inp

Expressions (3.5.3) and (3.5.4) indicate that the investigated quadripole has dispersion properties. Here it must be noted that for conjugate pulse responses (LFM signals) the law of variation of the frequency is a mirror law with respect to the law of variation of the frequency in the reference signal, and for the normal pulse responses, coinciding with the law of frequency variation in the reference signal.

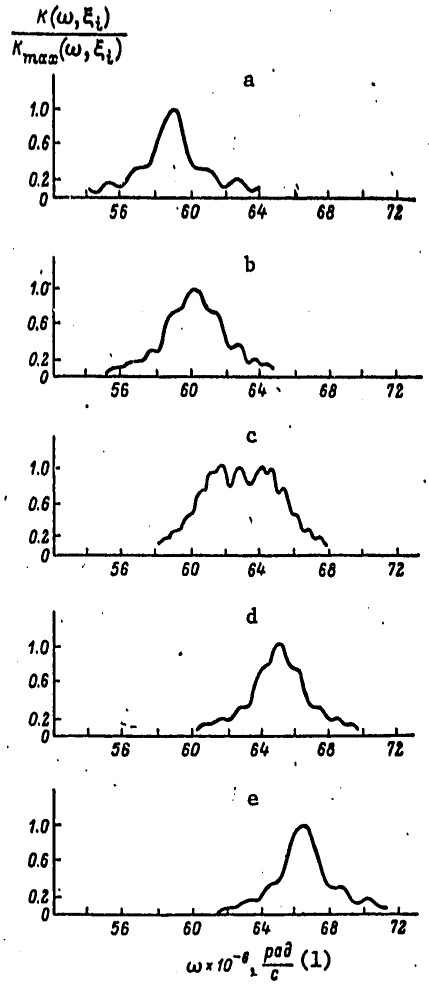

Figure 25. $K(\omega, \xi)$ surface cross sections. $P = 1$, $T_{ref} = 10$ microseconds, $T_{inp} = 20$ microseconds; $f_0 = 10$ megahertz, $2\Delta f_0 = 2$ megahertz for the LFM reference signal. ξ_i, microseconds: a -- 2, b -- 8, c -- 10-20, d -- 22, e -- 32.

Key: 1. radians/sec

Substituting (2.5.3) in (3.3.10), we obtain the expression for the complex conjugate transmission coefficient of the investigated quadripole.

Expressions (3,5,3), (3,5,4) and (3,3,10) permit the construction of surfaces corresponding to $g(\tau, \xi)$ and $K(\omega, \xi)$ for the given $s_{ref}(t)$, P, T_{ref} and T_{inp}.

Some surface cross sections $K(\omega, \xi)$ by the planes perpendicular to the plane (ξ, ω) and parallel to the ω-axis are presented in Figure 25. These cross sections -- the functions $K(\omega, \xi_1)$ -- correspond to the spectra of the LFM signals with different coefficients $m' = 2f_dT$, where f_d is the frequency deviation, T is the duration of the LFM signal [12].

The dependence of the frequency-amplitude characteristic of the parametric dispersion quadripole (the modulus of the transmission coefficient) on the observation time ξ_i is explained by the fact that the frequency properties of this quadripole are determined by the position of the elastic wave packet corresponding to the LFM signal in the apperture of the ALM I.

Thus, for the example presented in Figures 3.5.1, from $\xi_i = 0$ to $\xi_i \leq 10$ microseconds the elastic wave packet still did not completely go to the aperture of the ALM I, and the pass band of the quadripole is small. For 10 microseconds less than $\xi_i \leq 20$ microseconds, the entire elastic wave packet is in the aperture, and the frequency characteristics of the quadripole completely coincide with the amplitude and phase spectra of the reference signal. Then, as the elastic wave packet corresponding to the reference signal leaves the aperture, the pass band of the quadripole becomes more constricted. The phase-frequency characteristic of the quadripole undergoes the corresponding operations.

Analogous discussions and relations can also be presented for $T_{ref} > T_{inp}/P$.

Now let us consider the parametric quadripole, the functional diagram of which is presented in Figure 22. If the reference signal generator in the parametric quadripole shapes the LFM signal defined by (3.5.1), then considering (3.3.25) and (3.3.26), the pulse response for $T_{inp} > PT_{ref}$ is defined by the following expression in terms of the normal pulse responses:

$$g(\xi,\rho) =$$

$$= \begin{cases} B\cos\left[\omega_0\left(\xi-\rho_i-\frac{PT_{on}}{2}\right)-\frac{\beta_0}{2}\left(\xi-\rho_i-\frac{PT_{on}}{2}\right)^2\right] \\ \text{for } -T_{on} \leqslant \rho_i \leqslant 0 \text{ for } -(P-1)\rho_i \leqslant \xi \leqslant \rho_i + PT_{on}, \\ B\cos\left[\omega_0\left(\xi-\rho_i-\frac{PT_{on}}{2}\right)-\frac{\beta_0}{2}\left(\xi-\rho_i-\frac{PT_{on}}{2}\right)^2\right] \\ \text{for } 0 < \rho_i \leqslant T_{ax} \text{ for } \rho_i \leqslant \xi \leqslant \rho_i + PT_{on}, \\ B\cos\left[\omega_0\left(\xi-\rho_i-\frac{PT_{on}}{2}\right)-\frac{\beta_0}{2}\left(\xi-\rho_i-\frac{PT_{on}}{2}\right)^2\right] \\ \text{for } \underset{(2)}{T_{ax} < \rho_i \leqslant T_{ax} + T_{on}} \text{ for } \underset{(1)}{\rho_i \leqslant \xi \leqslant -(P-1)\rho_i + P(T_{ax} + T_{on})}. \end{cases} \qquad (3.5.5)$$

Key: 1. reference 2, input

It is possible to represent $g(\rho, \xi)$ in the following form in terms of a set of conjugate pulse responses:

$$g(\xi,\rho)=\begin{cases} B\cos\left[\omega_0\left(\xi_i-\rho-\frac{PT_{0n}}{2}\right)-\frac{\beta_0}{2}\left(\xi-\rho-\frac{PT_{0n}}{2}\right)^2\right] \\ \text{for } 0\leqslant\xi_i\leqslant(P-1)\,T_{0n} \text{ for } \frac{\xi_i}{P-1}\leqslant\rho\leqslant\xi_i, \\ B\cos\left[\omega_0\left(\xi_i-\rho\frac{PT_{0n}}{2}\right)-\frac{\beta_0}{2}\left(\xi_i-\rho-\frac{PT_{0n}}{2}\right)^2\right] \\ \text{for } (P-1)\,T_{0n}<\xi_i\leqslant T_{0n}+T_{ax} \text{ for } \xi_i-PT_{0n}\leqslant\rho\leqslant\xi_i, \\ B\cos\left[\omega_0\left(\xi_i-\rho-\frac{PT_{0n}}{2}\right)-\frac{\beta_0}{2}\left(\xi_i-\rho-\frac{PT_{0n}}{2}\right)^2\right] \\ \text{for } T_{0n}+T_{ax}<\xi_i\leqslant T_{ax}+PT_{0n} \text{ for } \xi_i-PT_{0n}\leqslant\rho\leqslant \\ \leqslant\frac{\xi_i}{P-1}+\frac{P}{P-1}(T_{ax}+T_{0n}). \end{cases} \qquad (3.5.6)$$

Key: 1. reference 2. inp

Thus, both the normal and the conjugate pulse responses are LFM signals. Consequently, the parametric quadripole has dispersion properties. Here both the normal and the conjugate pulse responses have a law of frequency variation the same as the law of frequency variation in the reference signal.

The conjugate complex transmission coefficient for the mirror image in time of the input signal of this parametric dispersion quadripole coincides with respect to its structure with the conjugate complex transmission coefficient of the quadripole (Figure 19).

The parametric dispersion quadripoles investigated above have the greatest practical significance for the reasons already mentioned. Accordingly, two possible versions of the construction of such quadripoles based on the correlative analysis acoustooptical devices are described in more detail. However, the methods of analysis are common to all types of such devices and do not depend on the form of the reference signal.

3.6. Time Scale Converters based on Acoustooptical Parametric Quadripoles

For the construction of the acoustooptic correlators and convolvers the device executed in accordance with the generalized structural diagram presented in Figure 17, as was pointed out above, must be supplemented by the time scale converter (TSC).

The time scale conversion is one of the linear conversions of electric signals frequently encountered in radioelectronics.

Thus, for example, for observation and analysis of wideband microwave signals using the electronic equipment existing at the present time, a device is needed to extend the time scale of the signal with simultaneous compression

of its spectrum, and preliminary compression of the time scale is required to process low-frequency hydroacoustic signals.

In addition, the time-scale converters (time transformers) are highly useful to study the fast nonelectric processes, for spectral and correlation analy s, for matching the transmission rate of the information with the parameters of the transmission and reception devices, and so on.

Interesting possibilities are opened up by the application of the TSC for shaping microwave signals. The pulse signal is generated in this case on intermediate frequency by one of the known methods (for example, using a passive ultrasonic delay line generator), and then it is fed to the TSC, from the output of which the microwave signal is picked up. Such an analysis of the modern state of the art of the equipment for time-scale conversion of electric signals, the TSC construction principles and some of the theoretical aspects of the problem can be found in references [44, 57].

In addition to the indicated papers, at the present time there are a significant number of publications devoted to the TSC, which indicates increased interest in the given field of engineering. The majority of the studies are performed as applied to the devices operating in the low and infralow frequency band. The studies of the devices used in the intermediate radiofrequency band are the subject of a significantly smaller number of papers. Of greatest interest among them are the articles [72, 123] which describe the TSC executed on the basis of the ultrasonic dispersion delay lines.

However, the requirements imposed on the ultrasonic dispersion delay lines (dispersion quadripoles) greatly limit the region of application of the TSC based on them. In particular, the magnitude of the product of the pass band width of the dispersion quadripole times the delay gradient corresponding to the linear section of the dispersion characteristic reaching several hundreds for the best ultrasonic delay lines must be significantly larger than the base of the signal at the TSC input (that is, much greater than the product of the signal spectral width times its duration). Therefore the TSC based on the ultrasonic delay lines obviously permit signals to be processed with a base not exceeding 100.

The possibility of the conversion of the nanosecond pulse time scales is illustrated in [44].

The TSC executed on the basis of segments of wave guides having dispersion properties near the critical frequency can find application in the microwave band [72]. However, along with the above-indicated restrictions, it is also necessary to take into account the fact that the duration of the processed signal will be determined by the length of the segment of the wave guide used as the dispersion quadripole, and in practice it will not exceed fractions of a microsecond.

The TSC executed on the basis of the acoustooptic parametric quadripoles are a new type of device of this class. Having high technical parameters (wide

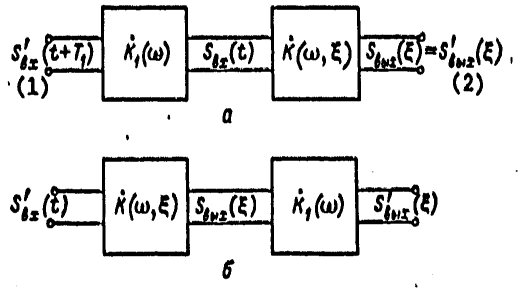

Figure 26. Structural diagrams of the TSC.

Key: 1. inp 2. out

band nature, the possibility of operating in both intermediate and high to superhigh frequency bands, and so on), they can find independent application. However, the studies of the acoustooptic TSC which were executed with the participation of the author have the goal of creating effective correlators.

Let us consider the possible structural diagrams of the acoustooptic time scale converters. In the case of a complex reference signal at the output of the acoustooptical parametric quadripole and electric signal is formed on a new time scale which corresponds either to the mutual correlation function of the input and the reference signals or their convolution. Consequently, when constructing the TSC, this parametric quadripole must be supplemented by some linear electric filter with constant or variable parameters included either at the input or at the output of the quadripole calculating that the output signal of this set will quite precisely reproduce the input signal on a new time scale (see Figure 26). If the corresponding parametric quadripole is used as the auxiliary electric filter, for example, the quadripole having the capacity to alter the time scale, the resultant alteration of the time scale can be quite large.

Let us also determine what requirements must be imposed on the linear electric filter supplementing the acoustooptic parametric quadripole,

We shall consider the structural diagram illustrated in Figure 21, a in which a linear electri filter with constant parameters is used as auxiliary.

When determining the requirements on the auxiliary linear electric filter we begin with the fact that the spectrum of the input signal of the TSC $s'_{inp}(t)$ and the spectrum of the output signal $s_{out}(\xi)$ observed in the new time scale must coincide with accuracy to the phase factor having a linear argument, that is, the following equality must be satisfied:

$$\dot{S}_{\substack{\text{вых}\\(1)}}(\omega) = D\dot{S}_{\substack{\text{вх}\\(2)}}(\omega)\exp(-j\omega\xi_0), \qquad (3.6.1.)$$

Key: 1. out 2. inp

where D is a dimensionless constant; $\dot{S}_{out}(\omega)$ is the spectral density of the output signal of the TSC observed in the new time scale; $\dot{S}_{inp}(\omega)$ is the spectral density of the input signal; ξ_0 is the delay time of the signal in the TSC reckoned on the new time scale.

For a fixed point in time ξ_i:

$$\dot{S}_{\substack{\text{вых}\\(1)}}(\omega) = \dot{S}_{\substack{\text{вх}\\(2)}}(\omega)\dot{K}_1(\omega)\dot{K}(\omega, \xi_i), \qquad (3.6.2)$$

Key: 1. out 2. inp

where $\dot{K}_1(\omega)$ is the complex transmission coefficient of the linear electric filter supplementing the parametric quadripole. Here

$$\dot{K}_1(\omega) = K_1(\omega)\exp[j\varphi_1(\omega)], \qquad (3.6.3)$$

where $K_1(\omega)$ and $\phi_1(\omega)$ are the frequency-amplitude and phase-frequency characteristics of the auxiliary electric filter, respectively.

If we select ξ_i in such a way that the elastic wave packet corresponding to the reference signal completely goes to the aperture of the corresponding light modulator (for example, for the system depicted in Figure 19, for $T_{inp} \geq PT_{ref}$ ξ_i must satisfy the condition $PT_{ref} \leq \xi \leq T_{inp}$), then

$$\dot{K}(\omega, \xi_i) = \underset{(1)}{BS_{\text{оп}}}(\omega)\exp[j\varphi_{\text{оп}}(\omega)], \qquad (3.6.4)$$

Key: 1. reference

where $S_{ref}(\omega)$ is the amplitude spectrum of the reference signal, $\phi_{ref}(\omega)$ is the phase spectrum of the reference signal.

Then, considering (3.6.2), (3.6.3) and (3.6.4), (3.6.1), will be written in the following form:

$$K_1(\omega)\exp[j\varphi_1(\omega)]BS_{\text{оп}}(\omega)\exp[j\varphi_{\text{оп}}(\omega)] = D\exp(-j\omega\xi_0). \qquad (3.6.5)$$

Hence,

$$\varphi_1(\omega) = -\omega\xi_0 - \varphi_{\text{оп}}(\omega), \qquad (3.6.6)$$

$$K_1(\omega) = \frac{D}{BS_{ss}(\omega)}. \qquad (3.6.7)$$

Thus, if we use the complex reference signal, as the auxiliary electric filter it is possible to use the matched filter [12, 25], correcting its frequency-amplitude characteristic in accordance with (3.6.7).

When selecting the parameters of the auxiliary electric filter it is also necessary to consider the variation of the time scale occurring in the parametric quadripole. Consequently, the filter supplementing the parametric quadripole must matched with the reference signal (considering the time scale conversion).

The initial data for the selection of the parameters of the auxiliary electric filter can be obtained from the table on page 76.*

It is natural that the introduction of the correction of the frequency-amplitude characteristic of this filter will lead to the fact that its pulse response will differ from the mirror image in time of the reference signal (considering the variable time scale).

It is interesting to note that when using the LFM reference signal with large product $m' = 2f_{d.ref}T_{ref}$ (where $f_{d.ref}$ is the frequency deviation of the reference signal), in practice correction of the frequency-amplitude characteristic of the auxiliary electric filter is not required as a result of the fact that the amplitude spectrum of this signal, which means, the frequency-amplitude characteristic of the filter matched with this signal, have almost rectangular envelopes. This fact again confirms the expediency of using the LFM signals as reference signals in the acoustooptic parametric quadripole.

Analogous arguments can be also be presented for the structural diagram depicted in Figure 26, b.

Here the auxiliary electric filter is also a filter matched with the reference signal (considering the variable time scale) supplemented by the device for correcting the frequency-amplitude characteristic.

The choice of the version of the structural diagram basically depends on the frequency band in which the given TSC is used and also the available element base. It is natural that both versions of the structural diagram of the TSC give identical results.

The application of the corresponding acoustooptic parametric quadripole as the auxiliary filter permits a significant increase in the coefficient of alteration of the time scale which this version of the TSC makes prospective. For this case it is possible to obtain the expressions similar to those which are presented above for the TSC with an auxiliary electric filter with constant parameters.

---

* [Translator's note: Page 76 of the original Russian not included in this translation.

Let us consider the operation of the time-scale compression device (time compressor) executed in accordance with the structural diagram presented in Figure 26, a. Let us assume that the LFM signal on the basis of which the TSC is constructed is used as the reference signal in the acoustooptic parametric quadripole, and the parametric quadripole is realized in accordance with the functional diagram presented in Figure 19.

It is obvious that here the auxiliary electric filter must have dispersion properties. Let us propose that the pulse response of this dispersion quadripole with constant parameters is defined by the expression

$$g_1(t, 0) = \cos\left[\omega_0\left(t - \frac{T_{д.к}^{(2)}}{2}\right) + \frac{\beta_{д.к}^{(1)}}{2}\left(t - \frac{T_{д.к}}{2}\right)^2\right].$$

Key: 1. dispersion quadripole
2. frequency deviation

for $0 \leq t \leq T_{\text{dispersion quadripole}}$, where $T_{\text{dispersion quadripole}}$ is the effective duration of the pulse response of the dispersion quadripole, $\beta_{\text{frequency deviation}} = 2\omega_{\text{frequency deviation}}/T_{\text{frequency deviation}}$, $\omega_{\text{freq. dev.}}$ is the frequency deviation in the pulse response.

Then finding the pulse response of the time scale compression device reduces to finding the signal at the output of the dispersion parametric quadripole on feeding the LFM signal to its input. The calculation can be performed based on the known expression

$$g_{\underset{(1)}{\text{ПВМ}}}(\gamma, \xi) = \int_{\tau_1}^{\tau_2} g_1(\tau - \gamma)\, g(\tau, \xi)\, d\tau, \qquad (3.6.8)$$

Key: 1. TSC

where γ is the time of application of the delta input.

Since in (3.6.8) the integration is carried out with respect to τ, the pulse response of the dispersion parametric quadripole $g(\tau_1, \xi)$ in this expression must be expressed in terms of the set of conjugate pulse responses in accordance with (3.5.4).

Let us assume that $PT_{\text{ref}} = T_{\text{dispersion quadripole}}$, $\beta_0 = \beta_{\text{frequency deviation}}$, and the duration of the input signal, the time scale of which must be converted is T'_{inp}. Then the effective duration of the signal at the input of the parametric quadripole with corresponding selection of the pass band width of the dispersion quadripole will be

$$T_{\text{вх}} \approx \underset{(1)}{T'_{\text{вх}}} + \underset{(2)}{T_{\text{д.с.}}} \tag{3.6.9}$$

Key: 1. inp 2. dispersion quadripole

Considering the region of assignment of $g(\tau, \xi)$ for $T_{ref} < T_{inp}/P$ (figure 20), it is possible to write (2.6.8) in the form

$$\underset{(1)}{g_{\text{ПВМ}}}(\gamma, \xi) = \int_{-\infty}^{+\infty} g_1(\tau - \gamma)\, g(\tau, \xi)\, \sigma(\xi - \tau)\, \sigma(\tau - \xi + PT_{\text{оп}})\, \sigma[(P+1)\tau - \underset{(2)}{-\xi + PT_{\text{оп}}}]\, \sigma\left(\frac{\xi}{P+1} - \tau + \frac{P}{P+1} T_{\text{вх}}\right) \sigma(\tau - \gamma)\, \sigma(\gamma - \tau + PT_{\text{оп}})\, d\tau, \tag{3.6.10}$$

Key: 1. TSC 2. reference

where

$$\sigma(x) = \begin{cases} 0 & \text{for } x < 0, \\ 1 & \text{for } x > 0. \end{cases} \tag{3.6.11}$$

For the LFM reference signal

$$g_{\text{ПВМ}}(\gamma, \xi) = B \int_{\tau_1}^{\tau_2} \cos\left[\omega_0\left(\tau - \gamma - \frac{PT_{\text{оп}}}{2}\right) + \frac{\beta_0}{2}\left(\tau - \gamma - \frac{PT_{\text{оп}}}{2}\right)^2\right] \times \cos\left[\omega_0\left(\tau - \xi + \frac{PT_{\text{оп}}}{2}\right) + \frac{\beta_0}{2}\left(\tau - \xi + \frac{PT_{\text{оп}}}{2}\right)\right] d\tau. \tag{3.6.12}$$

Expression (3.6.12) is easily reduced to the following [12]:

$$g_{\text{ПВМ}}(\gamma, \xi) = B \frac{\tau_2 - \tau_1}{2} \cdot \frac{\sin \frac{\beta_0}{2}(\xi - \gamma - PT_{\text{оп}})(\tau_2 - \tau_1)}{\frac{\beta_0}{2}(\xi - \gamma - PT_{\text{оп}})(\tau_2 - \tau_1)} \times \cos\left[\omega_0(\xi - \gamma + PT_{\text{оп}}) + \frac{\beta_0}{2}(\xi - \gamma - PT_{\text{оп}})(\tau_2 + \tau_1 - \gamma - \xi)\right]. \tag{3.6.13}$$

Defining τ_2 and τ_1 for the different γ and ξ, we find the region of assignment of $g_{TSC}(\gamma, \xi)$.

Considering the region of assignment of $g(\tau_1 \xi)$ and the effective duration $g_1(t - \gamma)$, we obtain:

for $-(P+1)T_{on} \leqslant \gamma \leqslant -PT_{on}$

$$\tau_1 = \frac{\xi - PT_{on}}{P+1},\ \tau_2 = \xi \text{ for } -T_{on} \leqslant \xi \leqslant \gamma + PT_{on},$$

$$\tau_1 = \frac{\xi - PT_{on}}{P+1},\ \tau_2 = \gamma + PT_{on} \text{ for } \gamma + PT_{on} < \xi \leqslant (P+1)\gamma + (P+2)T_{on};$$

for $-PT_{on} < \gamma \leqslant -T_{on}$

$$\tau_1 = \frac{\xi - PT_{on}}{P+1},\ \tau_2 = \xi \text{ for } -T_{on} \leqslant \xi \leqslant \gamma + PT_{on},$$

$$\tau_1 = \frac{\xi - PT_{on}}{P+1},\ \tau_2 = \gamma + PT_{on} \text{ for } \gamma + PT_{on} < \xi \leqslant PT_{on},$$

$$\tau_1 = \xi - PT_{on},\ \tau_2 = \gamma + PT_{on} \text{ for } PT_{on} < \xi \leqslant \gamma + 2PT_{on};$$

for $-T_{on} < \gamma \leqslant 0$

$$\tau_1 = \gamma,\ \tau_2 = \xi \text{ for } \gamma \leqslant \xi \leqslant (P+1)\gamma + PT_{on},$$

$$\tau_1 = \frac{\xi - PT_{on}}{P+1},\ \tau_2 = \xi \text{ for } (P+1)\gamma + PT_{on} < \xi \leqslant \gamma + PT_{on},$$

$$\tau_1 = \frac{\xi - PT_{on}}{P+1},\ \tau_2 = \gamma + PT_{on} \text{ for } \gamma + PT_{on} < \xi \leqslant PT_{on},$$

$$\tau_1 = \xi - PT_{on},\ \tau_2 = \gamma + PT_{on} \text{ for } PT_{on} < \xi \leqslant \gamma + 2PT_{on};$$

for $0 < \gamma \leqslant T_{ax} - PT_{on}$

$$\tau_1 = \gamma,\ \tau_2 = \xi \text{ for } \gamma \leqslant \xi \leqslant \gamma + PT_{on},$$

$$\tau_1 = \xi - PT_{on},\ \tau_2 = \gamma + PT_{on} \text{ for } \gamma + PT_{on} < \xi \leqslant \gamma + 2PT_{on};$$

for $T_{ax} - PT_{on} < \gamma \leqslant T_{ax} - (P-1)T_{on}$

$$\tau_1 = \gamma,\ \tau_2 = \xi \text{ for } \gamma \leqslant \xi \leqslant T_{ax},$$

$$\tau_1 = \gamma,\ \tau_2 = \frac{\xi + PT_{ax}}{P+1} \text{ for } T_{ax} < \xi \leqslant \gamma + PT_{on},$$

$$\tau_1 = \xi - PT_{on},\ \tau_2 = \frac{\xi + PT_{ax}}{P+1} \text{ for } \gamma + PT_{on} < \xi \leqslant (P+1)(\gamma + PT_{on}) - PT_{ax},$$

$$\tau_1 = \xi - PT_{on},\ \tau_2 = \gamma + PT_{on} \text{for } (P+1)(\gamma + PT_{on}) - PT_{ax} \xi \leqslant \gamma + 2PT_{on};$$

for $T_{ax} - (P-1)T_{on} < \gamma \leqslant T_{ax}$

$$\tau_1 = \gamma,\ \tau_2 = \xi \text{ for } \gamma \leqslant \xi \leqslant T_{ax},$$

$$\tau_1 = \gamma,\ \tau_2 = \frac{\xi + PT_{ax}}{P+1} \text{ for } T_{ax} \leqslant \xi \leqslant \gamma + PT_{on},$$

$$\tau_1 = \xi - PT_{on},\ \tau_2 = \frac{\xi + PT_{ax}}{P+1} \text{for } \gamma + PT_{on} < \xi \leqslant (P+1)T_{on} + T_{ax};$$

for $T_{ax} < \gamma \leqslant T_{ax} + T_{on}$

$$\tau_1 = \gamma,\ \tau_2 = \frac{\xi + PT_{ax}}{P+1} \text{ for } (P+1)\gamma - PT_{ax} \leqslant \xi \leqslant \gamma + PT_{on},$$

$$\tau_1 = \xi - PT_{on},\ \tau_2 = \frac{\xi + PT_{ax}}{P+1} \text{ for } \gamma + PT_{on} < \xi \leqslant (P+1)T_{on} + T_{ax}. \qquad (3.6.14)$$

The region of assignment of $g_{TSC}(\gamma, \xi)$ is illustrated in Figure 27. Expressions (3.6.13) and (3.6.14) determine the pulse response of the time compressor in terms of the set of normal pulse responses. Knowing the region of assignment of $g_{TSC}(\gamma, \xi)$, it is possible to write the pulse response in terms of the set of conjugate pulse responses and find the conjugate complex transmission coefficient of the device.

For an example, let us consider the passage of a rectangular radiopulse of duration T'_{inp} and with a carrier frequency of ω_0 through the time compressor, that is, let us determine the output signal of the device on feeding the following to its input:

$$s'_{\text{вх}}(t) = \begin{cases} \cos \omega_0 t & \text{for } 0 \leqslant t \leqslant T'_{\text{вх}}, \\ 0 & \text{for } t < 0 \text{ и } t > T'_{\text{вх}}. \end{cases} \tag{3.6.15}$$

(1)

Key: 1. out

Here

$$s_{\text{вых}}(\xi) = \int_{\gamma_1}^{\gamma_2} s_{\text{вх}}(\gamma)\, g_{\text{ПВМ}}(\gamma, \xi)\, d\gamma \tag{3.6.16}$$

(1) (2)

Key: 1. inp 2. TSC

The projection of the signal $s_{inp}(\gamma)$ of the gamma axis in Figure 27 is depicted by the segment OR.

Considering (3.6.14) for τ_1, τ_2 and ξ we have the following values: for $0 \leq \gamma \leq T'_{inp}$

$$\begin{array}{l} \tau_1 = \gamma, \tau_2 = \xi \text{ for } \gamma \leqslant \xi \leqslant \gamma + PT_{\text{оп}}, \\ \tau_1 = \xi - PT_{\text{оп}}, \ \tau_2 = \gamma + PT_{\text{оп}}, \text{ for } \gamma + PT_{\text{оп}} \leqslant \xi \leqslant \gamma + 2PT_{\text{оп}}. \end{array} \tag{3.6.17}$$

Then

$$g_{\text{ПВМ}}(\gamma, \xi) = \begin{cases} B\dfrac{\xi - \gamma}{2} \cdot \dfrac{\sin \beta_0 (\xi - \gamma - PT_{\text{оп}}) \dfrac{\xi - \gamma}{2}}{\beta_0 (\xi - \gamma - PT_{\text{оп}}) \dfrac{\xi - \gamma}{2}} \cos \psi_1 \text{ for } \gamma \leqslant \xi \leqslant \gamma + PT_{\text{оп}}, \\ B\left(\dfrac{\gamma - \xi}{2} + PT_{\text{оп}}\right) \dfrac{\sin \beta_0 (\xi - \gamma - PT_{\text{оп}}) \left(\dfrac{\gamma - \xi}{2} + PT_{\text{оп}}\right)}{\beta_0 (\xi - \gamma - PT_{\text{оп}}) \left(\dfrac{\gamma - \xi}{2} + PT_{\text{оп}}\right)} \times \\ \times \cos \psi_2 \text{ for } \gamma + PT_{\text{оп}} < \xi \leqslant \gamma + 2PT_{\text{оп}}, \end{cases} \tag{3.6.18}$$

where

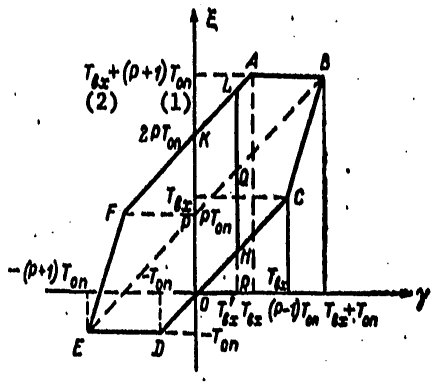

Figure 27. Region of assignment of $g_{TSC}(\gamma, \xi)$ of the time compressor for $T_{ref} < T_{inp}/P$.

Key: 1. ref 2. input

or

$$g_{\text{ПВМ}}(\gamma, \xi) = \begin{cases} g'_{\text{ПВМ}}(\gamma, \xi) \text{ for } \gamma \leqslant \xi \leqslant \gamma + PT_{\text{оп}} \\ g''_{\text{ПВМ}}(\gamma, \xi) \text{ for } \gamma + PT_{\text{оп}} \leqslant \xi \leqslant \gamma + 2PT_{\text{оп}}. \end{cases} \quad (3,6,19)$$

(1)

Key: 1. TSC

Thus,

$$s_{\text{вых}}(\xi) = \int_0^{\xi} s_{\text{вх}}(\gamma)\, g'_{\text{ПВМ}}(\gamma, \xi)\, d\gamma + \int_{\xi - PT_{\text{оп}}}^{\tau_{\text{вх}}} s_{\text{вх}}(\gamma)\, g'^{(1)}_{\text{ПВМ}}(\gamma, \xi)\, d\gamma +$$
$$+ \int_0^{\xi - PT_{\text{оп}}} s_{\text{вх}}(\gamma)\, g''_{\text{ПВМ}}(\gamma, \xi)\, d\gamma + \int_{\xi - 2PT_{\text{оп}}}^{\tau_{\text{вх}}} s_{\text{вх}}(\gamma)\, g''_{\text{ПВМ}}(\gamma, \xi)\, d\gamma =$$
$$= s'_{\text{вых}}(\xi) + s''_{\text{вых}}(\xi) + s'''_{\text{вых}}(\xi). \quad (3,6,20)$$

(2) (3) (4)

Key: (1) TSC
(2) output
(3) input
(4) ref.

Here

$$s'_{\text{вых}}(\xi) = B \int_0^{\xi} \cos \omega_0 \gamma \frac{\xi - \gamma}{2} \cdot \frac{\sin \beta_0 (\xi - \gamma - PT_{\text{оп}}) \frac{\xi - \gamma}{2}}{\beta (\xi - \gamma - PT_{\text{оп}}) \frac{\xi - \gamma}{2}} \times$$
$$\times \cos \left[\omega_0 (\xi - \gamma - PT_{\text{оп}}) + \beta_0 (\xi - \gamma - PT_{\text{оп}}) \frac{\xi - \gamma}{2} \right]. \quad (3,6,21)$$

Dropping the terms containing the frequency functions $2\omega_0$ under the integral sign [12], we obtain

$$s'_{вых}(\xi) = \frac{1}{2} B \int_0^{T'_{вх}} \frac{\sin \beta_0 (\xi - \gamma - PT_{он}) \frac{\xi - \gamma}{2}}{\beta_0 (\xi - \gamma - PT_{он})} d\gamma \cos \omega_0 (\xi - PT_{он}) \qquad (3.6.22)$$

for $0 \leq \xi \leq PT_{ref}$.

Analogously,

$$s''_{вых}(\xi) = \frac{1}{2} B \left[\int_{\xi - PT_{он}}^{T'_{вх}} \frac{\sin \beta_0 (\xi - \gamma - PT_{он}) \frac{\xi - \gamma}{2}}{\beta_0 (\xi - \gamma - PT_{он})} d\gamma + \right.$$

$$\left. + \int_0^{\xi - PT_{он}} \frac{\sin \beta_0 (\xi - \gamma - PT_{он}) \left(\frac{\gamma - \xi}{2} + PT_{он} \right)}{\beta_0 (\xi - \gamma - PT_{он})} d\gamma \right] \cos \omega_0 (\xi - PT_{он}) \qquad (3.6.23)$$

for $PT_{он} < \xi \leqslant 2PT_{он}$,

$$s''_{вых}(\xi) = \frac{1}{2} B \int_{\xi - 2PT_{он}}^{PT'_{вх}} \frac{\sin \beta_0 (\xi - \gamma - PT_{он}) \left(\frac{\gamma - \xi}{2} + PT_{он} \right)}{\beta_0 (\xi - \gamma - PT_{он})} d\gamma \cos \omega_0 (\xi - PT_{он})$$

for $2PT_{он} < \xi \leqslant 2PT_{он} + T'_{вх}$. (3.6.24)

If $P = 1$ and $T'_{in\,p} = T_{ref}$,

$$S_{вых}(\xi) =$$

$$= \begin{cases} \frac{1}{2} B \int_0^{\xi} \frac{\sin \beta_0 (\xi - \gamma - T_{он}) \frac{\xi - \gamma}{2}}{\beta_0 (\xi - \gamma - T_{он})} d\gamma \cos \omega_0 (\xi - T_{он}) \text{ for } 0 \leqslant \xi \leqslant T_{он}, \\ \frac{1}{2} B \left[\int_{\xi - T_{он}}^{T_{он}} \frac{\sin \beta_0 (\xi - \gamma - T_{он}) \frac{\xi - \gamma}{2}}{\beta_0 (\xi - \gamma - T_{он})} d\gamma + \right. \\ \left. + \int_0^{\xi - T_{он}} \frac{\sin \beta_0 (\xi - \gamma - T_{он}) \left(\frac{\gamma - \xi}{2} + T_{он} \right)}{\beta_0 (\xi - \gamma - T_{он})} d\gamma \right] \times \\ \times \cos \omega_0 (\xi - T_{он}) \text{ for } T_{он} < \xi \leqslant 2T_{он}, \\ \frac{1}{2} B \int_{\xi - 2T_{он}}^{T_{он}} \frac{\sin \beta_0 (\xi - \gamma - T_{он}) \left(\frac{\gamma - \xi}{2} + T_{он} \right)}{\beta_0 (\xi - \gamma - T_{он})} d\gamma \cos \omega_0 (\xi - T_{он}) \\ \text{for } 2T_{он} < \xi \leqslant 3T_{он}. \end{cases} \qquad (3,6,25)$$

Expression (2,6,25) describes the signal, the shape of the envelope which approaches rectangular. The degree of this approximation depends strongly on the value of $m' = \omega_{\text{frequency deviation}} T_{\text{dispersion quadripole}}/\pi$ [25].

The device for shaping the inverse time scale (the device for shaping the mirror image of the signal in time) as follows from the table on page 76, can be executed on the basis of the acoustooptic quadripoles in which the elastic wave packet corresponding to the reference signal (or its image) is shifted with a velocity greater than the velocity of shifting the elastic wave packet corresponding to the input signal (or its image). Here both optical signals must move in the same direction.

Let us consider the device for shaping the inverse time scale based on the acoustooptic quadripole with an enlarged reference signal image (Figure 22). Here we shall analyze the structural diagram presented in Figure 26, a.

When using the LFM reference signal, the auxiliary quadripole must have dispersion properties.

Thus, if

$$s_{on}(t-\tau-T_{ax}) = \cos\left[\omega_{on}\left(t-\tau-\frac{T_{on}}{2}-T_{ax}\right)+\frac{\beta_{on}}{2}\left(t-\tau-\frac{T_{on}}{2}-T_{ax}\right)^2\right] \tag{3,6,26}$$

for $0 \leqslant t-T_{ax}-\tau \leqslant T_{on}$

and

$$g(\tau, \xi) = B\cos\left[\omega_0\left(\tau+\xi-T_{ax}-\frac{PT_{on}}{2}\right)+\frac{\beta_0}{2}\left(\tau+\xi-T_{ax}-\frac{PT_{on}}{2}\right)^2\right], \tag{3.6.27}$$

the pulse response of the auxiliary dispersion quadripole

$$g_1(t) = \cos\left[\omega_0\left(t-\frac{T_{д.з}}{2}\right)+\frac{\beta_{д.з}}{2}\left(t-\frac{T_{д.з}}{2}\right)^2\right] \tag{3.6.28}$$

for $0 \leq t \leq T_{\text{dispersion quadripole}}$.

As has already been done above, let us define the pulse response of the device for shaping the time scale using the known expression

$$g_{\text{ПВМ}}(\gamma, \xi) = \int_{-\infty}^{+\infty} g_1(\tau-\gamma)\, g(\tau, \xi)\, d\tau, \tag{3,6,29}$$

where γ is the time of application of the delta input.

Let us propose that $PT_{\text{ref}} = T_{\text{dispersion quadripole}}$, and $\beta_{\text{dispersion quadripole}} = \beta_0$. In addition, we shall consider that the effective duration of the signal at the input of the parametric quadripole

$$T_{вх} \approx T'_{вх} + PT_{оп}, \tag{3,6,30}$$

where T'_{inp} is the duration of the signal for which the mirror image in time is formed,

The nonstationarity of the properties of the parametric quadripole when calculating the pulse response of the TSC will be taken into account using the expression

$$g_{ПВМ}(\gamma, \xi) \int_{-\infty}^{+\infty} \sigma(\tau-\gamma)\,\sigma(\gamma-\tau+PT_{оп})\,\sigma\left(\frac{\xi}{p-1}-\tau+T_{вх}\right)\times$$
$$\times\sigma\left(\tau-\frac{\xi-T_{вх}-PT_{оп}}{P-1}\right)\cdot\sigma(\tau-T_{вх}+\xi)\cdot\sigma(-\tau+\xi+T_{вх}+PT_{оп})\times$$
$$\times g_1(\tau-\gamma)\,g(\tau,\xi)\,d\tau, \tag{3,6,31}$$

where

$$\sigma(x)=\begin{cases}1 & \text{for } x\geqslant 0,\\ 0 & \text{for } x<0.\end{cases} \tag{3,6,32}$$

Assigning various values to ξ and γ, we obtain the corresponding integration limits τ_1 and τ_2. Here

$$g_{ПВМ}(\gamma,\xi)\approx B\frac{\tau_2-\tau_1}{2}\cdot\frac{\sin\frac{\beta_0}{2}(T_{вх}-\gamma-\xi)(\tau_2-\tau_1)}{\frac{\beta_0}{2}(T_{вх}-\gamma-\xi)(\tau_2-\tau_1)}\times$$
$$\times\cos\left[\omega_0(T_{вх}-\gamma-\xi)+\frac{\beta_0}{2}(T_{вх}-\gamma-\xi)(\tau_2+\tau_1+\xi_1-\gamma-T_{вх}-PT_{оп})\right]. \tag{3.6.33}$$

The region of assignment of $g_{TSC}(\gamma, \xi)$ of the device for shaping the inverse time scale is shown in Figure 28,

Knowing the region of assignment of $g_{TSC}(\gamma, \xi)$ and its analytical expression, it is possible to obtain the relations for determining the conjugate complex transmission coefficient of the device with respect to the mirror image in the time of the input signal.

The photographs presented in Figure 29 illustrate the operation of the time compressor in accordance with the structural diagram indicated in Figure 26,a on the basis of the dispersion acoustooptic quadripole,

This quadripole is the simplest convolver (see Figure 15) assembled on the basis of the MTO-1000 photoobjective with mercury tube as the light source.

The acoustic light modulators are glass cells with distilled water in which ultrasonic waves were excited by electroacoustic converters made of piezoceramics. The pass band width of the ALM is 2 megahertz with an average frequency f_0 = 10 megahertz. A photomultiplier with electric band filter as load was used as the photodetector.

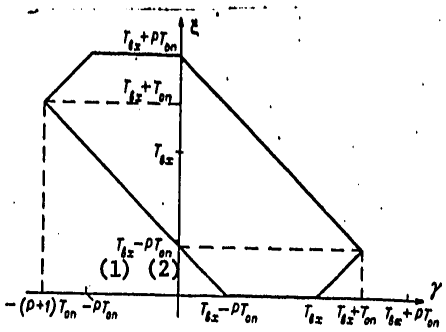

Figure 28. Region of assignment of $g_{TSC}(\gamma, \xi)$ of the device for shaping the inverse time scale

Key: 1. inp 2. ref

The linear frequency modulated radio pulse was fed to one of the inputs of the convolver with the following parameters: average frequency f_0 = 10 megahertz, frequency deviation $2f_d$ = 2 megahertz, duration T = 10 microseconds, law of variation of frequency in the pulse, "increasing."

The dispersion ultrasonic delay line on surface waves was used as the auxiliary dispersion quadripole with constant parameters, the pulse response of which has the following parameters: average frequency f_0 = 10 megahertz, frequency deviation $2f_d$ = 2 megahertz, duration T= 10 microseconds, law of frequency variation, "decreasing."

A rectangular radio pulse of 10 microseconds duration, the filling frequency of which could be varied, was fed to the input of the time compressor. Figure 26, a shows an oscillogram of the input radio pulse with filling frequency of 10 megahertz. The oscillogram of the signal at the output of the time compressor is illustrated in Figure 26, b.

The output signal has almost rectangular envelope. Its duration is 5 microseconds, and filling frequency, 20 milliseconds.

The photographs presented in Figure 30 demonstrate the operation of the time scale extension device (the time expander). This device is executed on the basis of a parametric quadripole, the functional diagram of which is presented

in Figure 24, A helium-neon laser was used as the light source. The acoustic light modulators were made of STF-3 and BF-28 type optical glass (the speed of the longitudinal elastic waves was $3,5 \cdot 10^6$ and $4,35 \cdot 10^6$ mm/sec, respectively). The elastic waves in the modulators were excited by electroacoustic converters made of lithium niobate. The average pass band frequencies of two ALM are 50 megahertz. The pass band width somewhat exceeds 12 megahertz. A rectangular pulse lasting 0,5 microseconds with a filling frequency of 47.5 megahertz was used as the reference signal. This signal was fed to the STF-3 optical glass ALM. The signal, the time scale of which must be expanded reached the input of the BF-28 optical glass ALM. For illustration of the operation of the time expander, and exponential radio pulse lasting 2.5 microseconds with a filling frequency of 59 megahertz was used as the processed signal.

The new time scale formed by the devices -- $\xi = 0.196\ t$ -- corresponds to an expansion coefficient of the time scale of 5,1.

Inasmuch as for illustration of the operation of the time scale expansion device a simple reference signal -- rectangular radio pulse -- was used, an auxiliary quadripole was not introduced into the system. In Figure 30, a an oscillogram of the input radio pulse is presented, and in Figure 30, b, the signal from the output of the TSC. Since the rectangular reference radio pulse had finite duration commensurate with the duration of the input signal, the pulse at the output of the TSC has extended fronts.

The device for extending the time scale described above can be used to shape the mirror image of the signal in time with simultaneous expansion of the time scale. For this purpose it is necessary to feed the reference signal to the ALM in which the propagation rate of the elastic waves is higher, that is, to the ALM made of BF-28 glass.

An exponential radio pulse of 2.5 microsecond duration with filling frequency of 47.5 megahertz (Figure 31,a) was used as the input signal. This signal was fed to the ALM made of STF-3 glass. A reference signal in the form of a square radio pulse lasting 1 microsecond with a filling frequency of 59 megahertz was fed to the other ALM with a delay equal to the duration of the input signal. In Figure 31, b, the output signal of the device which shapes the inverse expanded time scale with the expansion coefficient 4.13 is shown.

Another version of the device for shaping the inverse time scale based on a parametric quadripole, the functional diagram of which is presented in Figure 22 is made in accordance with the structural diagram illustrated in Figure 26, a. A helium-neon laser was used as the light source 1. The collimators 3 and the objective 4 are spherical mirrors with focal lengths of 0.5 meters; the objectives 5 and 6 are spherical mirrors with focal lengths equal to 1 meter. Thus, the magnification factor of the optical system 4, 5 is equal to 2, which makes it possible to shape the mirror image of the signals in real time. The ALM are made of STF-3 type optical glass with electroacoustic converters made of lithium niobate which excites longitudinal elastic waves. The traveling wave mode is achieved by oblique cutting of the end of the

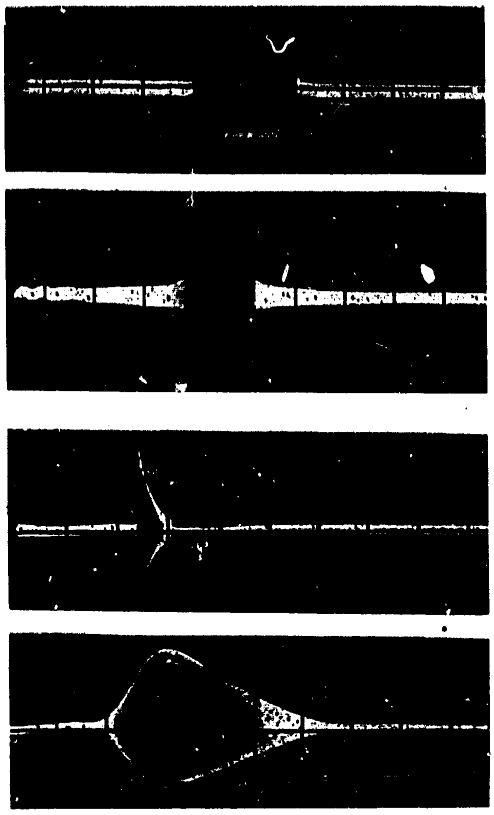

Figure 29. Oscillograms illustrating the operation of the time compressor. Scanning scale 5 microseconds/cm. a -- signal at the input, b -- signal at the output.

Figure 30. Oscillograms illustrating the operation of the time scale expansion device. Scanning scale 4 microseconds/cm, a -- signal the input, b -- signal at the output.

sound guide of the ALM. Here the ALM 10 has the following parameters: average pass band frequency 24 megahertz, pass band width 4 megahertz. For the ALM 8 the average pass band frequency is 12 megahertz, and the pass band width is 2 megahertz.

An ultrasonic dispersion delay line based on surface waves, the pulse response of which has the following parameters was used as the auxiliary electric

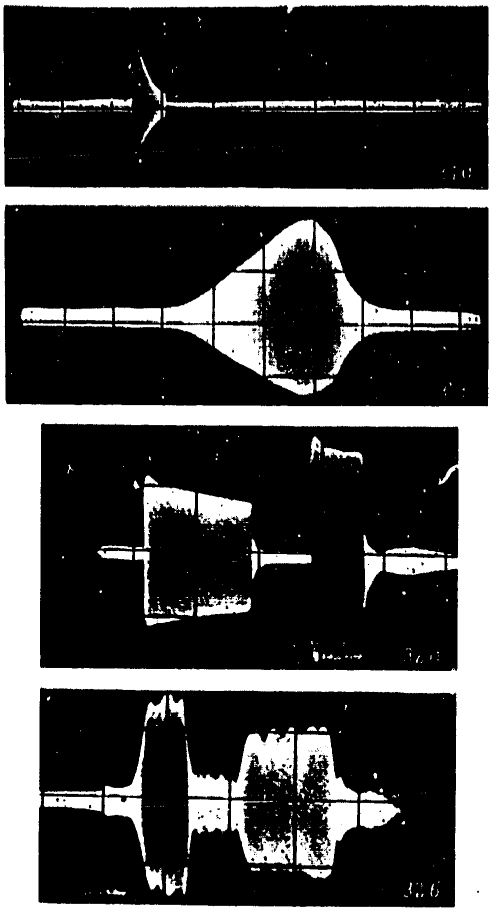

Figure 31. Oscillograms illustrating the operation of the device for shaping the inverse expanded time scale. Convolution scale 4 microseconds/cm, a -- signal at the input, b -- signal at the output.

Figure 32. Oscillograms illustrating the operation of the device for shaping the inverse time scale in real time. a -- signal at the input, b -- signal at the output.

filter in the device; response time -- $T_{\text{dispersion quadripole}}$ = 10 microseconds, frequency deviation $2f_d$ = 2 megahertz, average frequency f_0 = 12 megahertz, law of frequency variation, "increasing."

The ultrasonic dispersion delay line based on surface waves was used as the "passive" reference signal generator with linear frequency modulation. This generator shapes the LFM signal with the following parameters: signal duration T_{ref} = 5 microseconds, frequency deviation $2f_{d,ref}$ = 4 megahertz, average frequency f_{ref} = 24 megahertz.

The device makes it possible to shape the mirror image in time of the signals with a duration of up to 20 microseconds on carrier frequencies of 12 megahertz with a spectral width to 2 megahertz. The operation of the TSC is illustrated by the oscillograms presented in Figure 32. The input signal is a sequence made up of two pulses of different duration (10 and 5 microseconds) and different amplitude with filling frequency of 12 megahertz. The output signal corresponds quite well to the mirror image in time of the input signal.

3.7. Selection of the Version of the Acoustooptic Correlator

The analysis of the generalized structural diagram of the acoustooptic device which is depicted in Figure 17 indicates that different versions of the correlators are possible. Being given the required time scale of formation of the output signal, selecting the corresponding acoustic interaction media and parameters of the optical assemblies, the initial data are determined for selecting the characteristics of the time scale converter. In this case the different combinations of values of P and Q (see item 3.3) will permit us to obtain the same output effect. Thus, the developer of the corresponding equipment is faced with the problem of selecting the optimal version of the correlator.

The optimal version of the correlator can be the one in which the size of the aperture of the ALM is minimal in the direction of propagation of the elastic wave. The introduction of this criterion is caused both by the presence of damping of elastic waves in the acoustooptic interaction medium and the shortage of high-quality objectives have large apertures.

The number of versions of the acoustooptic correlators for the given initial data is comparatively low. Therefore the choice of the optimal version can be made by the sorting method.

If no special requirements are imposed on the time scale of the output signal of the correlator, the correlator made up of the simplest acoustooptic convolver 1 and the TSC forming the mirror image in time of one of the signals in real time (Figure 33) can be recognized as optimal in the above-indicated sense. Here the signal reaching the input II of the correlator is delayed by the device 2 for the time T_0, during which the mirror image of the signal reaching the input I is formed.

In this device the acoustooptic convolver is executed in accordance with the special diagram depicted in Figure 15. Figure 34 shows one of the possible optical systems of the correlator. The upper part of the system is the optical system of the device for shaping the inverse time scale [28], and the lower part of the diagram, the optical system of the convolver.

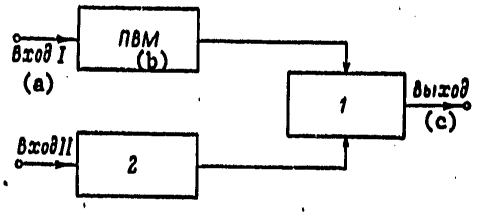

Figure 33. Structural diagram of a version of constructing a radiosignal correlator based on an acoustooptic convolver.

Key: a. input... b. TSC c. output

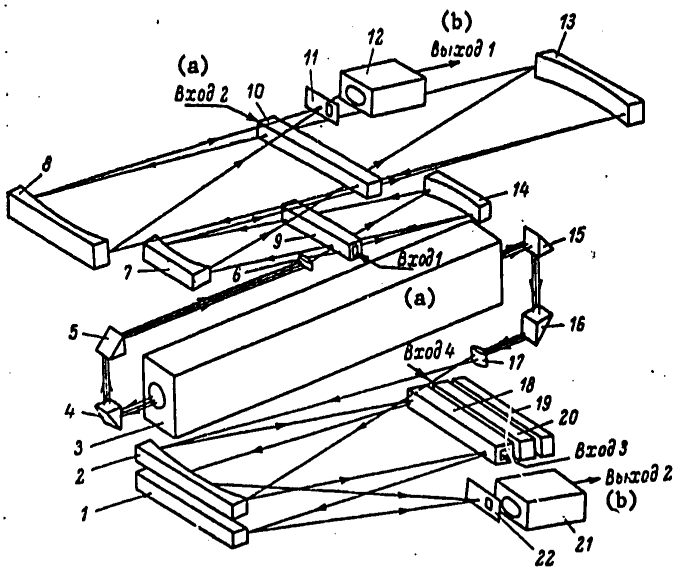

Figure 34. Optical system of the correlator.

Key: a. input... b. output...

The light source 3 for which the laser is used creates a light flux used both in the TSC and in the convolver. The prisms 4 and 5 and also 15 and 16 are used to change the direction of propagation of the light waves. The optical system of the TSC includes the condenser 6, spherical mirrors 7, 8, 13 and 14, the AMC 9 and 10, the slit diaphragm 11 and the photomultiplier 12 with band electric filter as load. The mirrors 7 and 14 have focal lengths equal to 500 mm, and 8 and 13, 1000 mm. This provides for a twofold magnification of the reference signal image fed to the ALM 9, that is, the input I.

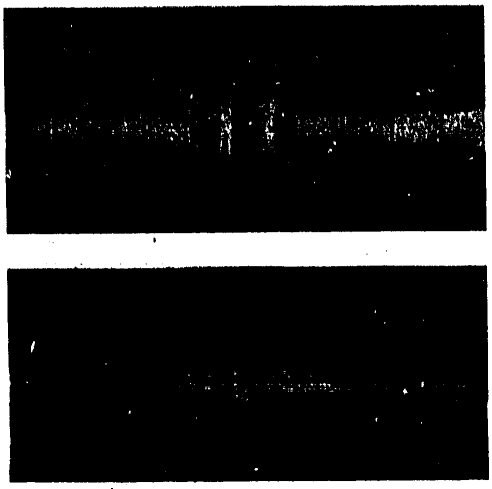

Figure 35. Oscillogram of the output signal of the correlator corresponding to the autocorrelation function of a series of two radio pulses of different duration.

Figure 36. Oscillogram of the output signal of the correlator corresponding to the autocorrelation function of a "segment" of a noise signal.

The optical system of the convolver [89] includes the condenser 17, the spherical mirrors 1 and 2 which are combined in 1 mirror, the ALM 18 and 20, the flat mirror 19, the slit diaphragm 22 and the photomultiplier 21 with band electric filter and load. The traveling wave mode has been created as a result of the oblique cut of the tip of the ALM sound guide in it.

Figures 35 and 36 show the oscillograms illustrating the operation of the device in which the acoustic light modulators are made of STF-3 type optical glass with electroacoustic converters made of lithium niobate (Q = 1) exciting longitudinal elastic waves.

Thus, in Figure 35 we have the oscillogram of the output signal of the correlator corresponding to the autocorrelation function of the sequence of two radio pulses with rectangular envelope of 4 microseconds duration and 3 microseconds separated by an interval of 3 microseconds with a carrier frequency of 12 megahertz. As a result of counterpropagation of the elastic waves in the ALM of the convolver the autocorrelation function is shaped in unreal time, and the carrier frequency of the output signal is 24 megahertz.

Figure 36 shows the autocorrelation function of the "segment" of the noise signal of 10 microseconds duration for a spectral width of 2 megahertz.

BIBLIOGRAPHY

1. V. A. Andreyev, S. V. Kulakov, B. P. Razzhivin, et al., "Multichannel Wave Guide Ultrasonic Light Modulator," USSR Author's Certificate No 393791, BYUL. IZOBRET (Invention Bulletin), No 33, 1973.

2. P. A. Bakut, V. G. Chumak, "Optoacoustic Autocorrelator for an LFM Signal," RADIOTEKHNIKA I ELEKTRONIKA (Radio Engineering and Electronics), No 9, 1970, pp 1916-1921.

3. L. D. Bakhrakh, A. P. Kurochkin, S. G. Rudneva, "Use of an Ultrasonic Light Modulator for Parallel Processing of the Signals of an Antenna Array," VOPROSY RADIOELEKTRONIKI. SERIYA OT (Problems of Radioelectronics. Optical Engineering Series), No 1, 1972, pp 36-48.

4. G. S. Belikova, L. M. Belyayev, N. P. Golovey, et al., "Growing Rubidium and Cesium Biphthalate Crystals and the Investigation of their Optoacoustic and nonlinear Optical Properties," KRISTALLOGRAFIYA (Crystallography), Vol 19, No 3, 1974, pp 566-572.

5. L. Bergman, UL'TRAZVUK I YEGO PRIMENENIYE V NAUKE I TEKHNIKE (Ultrasound and Its Application in Science and Engineering), Moscow, IIL, 1957, 726 p.

6. V. A. Besekerskiy, Ye. P. Popov, TEORIYA SISTEM AVTOMATICHESKOGO REGULIROVANIYA (Theory of Automated Control Systems), Moscow, Nauka, 1972, 768 p.

7. S. V. Bogdanov, I. I. Zubrinov, D. V. Sheloput, "Study of Materials Prospective for Acoustooptic Devices," IZV. AN SSSR. SER. FIZIKA (News of the USSR Academy of Sciences, Physics Series), Vol 35, No 5, 1971, pp 1013-1014.

8. M. Born, E. Vol'f, OSNOVY OPTIKI (Fundamentals of Optics), Moscow, Nauka, 1970, 856 pp.

9. D. Ye. Vakman, SLOZHNYYE SIGNALY I PRINTSIP NEOPREDELENNOSTI V RADIOLOKATSII (Complex Signals and the Principle of Indeterminancy in Radar), Moscow, Sovetskoye radio, 1965, 304 pp.

10. V. T. Gibriyelyan, V. V. Kludzin, S. V. Kulakov, et al., "Elastic and Photoelastic Properties of Single Lead Molybdate Crystals," FIZIKA TVERDOGO TELA (Solid State Physics), Vol 17, 1975, pp 603-604.

11. B. Gold, Ch. Reyder, TSIFROVAYA OBRABOTKA SIGNALOV (Digital Processing of Signals), Moscow, Sovetskoye radio, 1973, 672 pp.

12. I. S. Gonorovskiy, RADIOTEKHNICHESKIYE TSEPI I SIGNALY (Radio Engineering Circuits and Signals), Moscow, Sovetskoye radio, 1971, 672 pp.

13. G. D'Angelo, LINEYNYYE SISTEMY S PEREMENNYMI PARAMETRAMI (Linear Systems with Variable Parameters), Moscow, Mashinostroyeniye, 1974, 288 pp.

14. S. A. Zabuzov, V. V. Kludzin, S. V. Kulakov, et al., "Ultrasonic Solid State Light Modulators for Optical Data Processing Systems," PROBLEMY GOLOGRAFII (Problems of Holography), Moscow, MIREA, No 2, 1973, pp 156-159.

15. V. V. Karavayev, Z. I. Fayzulin, "Theoretical Analysis of Some Optoacoustic Systems for Compression of LFM Radiosignals," TRUDY RADIOTEKHNICHESKOGO INSTITUTA AN SSSR (Works of the Radio Engineering Institute of the USSR Academy of Sciences, No 5, 1971, pp 125-141.

16. A. M. Kiryukhin, O. D. Moskalets, G. K. Ul'yanov, "Dispersion Spectral Analyzer of Video and Radio Signals," TRUDY LIAP (Works of the LIAP Institute), No 64, 1969, pp 40-52.

17. V. V. Kludzin, "Photoelastic Constants of $LiNbO_3$ Crystals," FIZIKA TVERDOGO TELA (Solid State Physics), Vol 13, No 2, 1971, pp 651-653.

18. V. V. Kludzin, "Study and Development of Ultrasonic Solid State Light Modulators for Radio Signal Processing Devices," Author's Review of Candidate's Dissertation, LIAP, 1972.

19. V. V. Kludzin, "Characteristics of the Variation in Light Intensity in a Diffraction Order depending on the Angle of Incidence of the Light Flux on the Surface of an Ultrasonic Light Modulator," IZV. VYSOV. RADIOFIZIKA (News of the Institutions of Higher Learning. Radiophysics, Vol 17, No 2, 1974, pp 261-264.

20. V. V. Kludzin, S. V. Kulakov, B. P. Razzhivin, "Ultrasonic Light Modulators in Optical Data Processing Systems," OPTICHESKIYE METODY OBRABOTKI INFORMATSII (Optical Methods of Data Processing), Leningrad, Nauka, 1974, pp 134-141.

21. V. V. Kludzin, S. V. Kulakov, B. P. Razzhivin, et al., "Possibility of Applying Heavy Flints for Ultrasonic Light Modulation," OPTIKO-MEKHANICHESKAYA PROMYSHLENNOST' (Opticomechanical Industry), No 1, 1972, pp 3-6.

22. G. S. Kondratenkov, OBRABOTKA INFORMATSII KOGERENTNYMI OPTICHESKIMI SISTEMAMI (Data Processing by Coherent Optical Systems), Moscow, Sovetskoye radio, 1972, 208 pp.

23. E. M. Krupitskiy, V. S. Lobach, T. N. Sergiyenko, et al., "High-Speed Acoustooptic Radio Signal Spectral Analyzer," PRIBORY I TEKHNIKA EKSPERIMENTA (Experimental Instruments and Techniques), No 2, 1975, pp 188-189.

24. A. G. Kuzin, S. V. Kulakov, "High-Frequency Acoustooptic Spectral Analyzer," AKUSTOOPTICHESKIYE USTROYSTVA OBRABOTKI SIGNALOV (MEZHVUZOVSKIY SBORNIK NAUCHNYKH TRUDOV) (Acoustooptic Devices for Signal Processing (Interuniversity Collection of Scientific Papers)), LETI Institute, pp 10-14.

25. Ch. Kuk, M. Bernfel'd, RADIOLOKATSIONNYYE SIGNALY (Radar Signals), Moscow, Sovetskoye radio, 1971, 568 pp.

26. S. V. Kulakov, "Signal Conversion by the Elements of an Optoacoustic Correlator with Amplitude Diffraction Grating as the Reference Signal," TRUDY LIAP (Works of the LIAP Institute), No 64, 1974, pp 82-86.

27. S. V. Kulakov, "Theory of Optoacoustic Correlator with Enlarged Image of the Reference Signal," PRIKLADNYYE ZADACHI DIFRAKTSII I RASSEYANIYA RADIOLOKATSIONNYKH SIGNALOV I VOPROSY IKH RASPOZNAVANIYA (Applied Problems of Diffraction and Scattering of Radar Signals and the Problems of their Recognition), Leningrad, SZPI, 1974, pp 82-86.

28. S. V. Kulakov, V. V. Kludzin, V. I. Yezhov, "Acoustooptic Radio Signal Time Scale Converters," GOLOGRAFIYA I OBRABOTKA INFORMATSII (Holography and Data Processing), Leningrad, Nauka, 1976, pp 125-134.

29. S. V. Kulakov, M. V. Leykin, A. O. Lyubich, "Problem of Constructing an Optoacoustic Signal Processing Device," TRUDY LIAP (Works of the LIAP Institute), No 45, 1965, pp 71-74.

30. S. V. Kulakov, O. D. Moskalets, B. P. Razzhivin, "Some Problems of the Theory of the Optoacoustic Spectral Analyzer," TRUDY LIAP, No 64, 1969, pp 96-108.

31. S. V. Kulakov, B. P. Razzhivin, S. P. Semenov, et al., "Optoacoustic Correlator Processing of FM Radio Pulses with Conversion of their Image Spectra," TRUDY LIAP, No 64, 1969, pp 109-113.

32. S. V. Kulakov, B. P. Razzhivin, S. I. Sokolov, et al., "Optoacoustic Correlation Spectral Analyzer," USSR Author's Certificate No 337730, BYUL. IZOBRET. (Invention Bulletin), No 15, 1973.

33. S. V. Kulakov, B. P. Razzhivin, S. I. Sokolov, et al., "Device for Shaping a Mirror Image in Time of a Processed Signal," USSR Author's Certificate No 374633, BYUL. IZOBRET., No 15, 1973.

34. S. V. Kulakov, B. P. Razzhivin, D. V. Tigin, "Some Problems of the Theory of an Optoacoustic Radio Signal Correlator," PROBLEMY GOLOGRAFII (Problems of Holography), Moscow, MIREA, No 2, pp 56-60.

35. S. V. Kulakov, B. P. Razzhivin, D. V. Tugin, "Dispersion Spectral Analyzer Based on an Optoacoustic Correlator," RASSEYANIYE I DIFRAKTSIYA RADIOLOKATSIONNYKH SIGNALOV I IKH INFORMATIVNOST' (Dispersion and Diffraction of Radar Signals and their Informativeness)_ Leningrad, SZPI, No 2, 1976, pp 84-87.

36. S. V. Kulakov, B. P. Razzhivin, D. V. Tigin, et al., "Application of the Theory of Linear Electric Circuits to the Analysis of a Simple Optical LFM Radio Pulse Compression Filter," PROBLEMY GOLOGRAFII, Moscow, MIREA, No 2, 1973, pp 40-50.

37. S. V. Kulakov, B. P. Razzhivin, D. V. Tigin, et al., "Dispersion Analyzer of the Pulse Signal Spectrum based on the Optoacoustic LFM radio pulse Compression Filter," PROBLEMY GOLOGRAFII, Moscow, MIREA, No 2, 1973, pp 51-55.

38. S. V. Kulakov, B. P., Razzhivin, D. V. Tigin, et al., "Optoacoustic Radio Signal Correlator," USSR Author's Certificate No 482702, BYUL. IZOBRET. No 32, 1975.

39. S. V. Kulakov, D. V. Tigin, "Shaping the Image of the Processed Signal in Optoacoustic Devices based on Light Diffraction on Ultrasound," TEZISY DOKLADOV VII VSESOYUZNOY AKUSTICHESKOY KONFERENTSII (Topics of Reports of the 7th All-Union Acoustics Conference), Leningrad, 1971, pp 106.

40. G. S. Landsberg, OPTIKA (Optics), Moscow-Leningrad, Gostekhizdat, 1947, 631 pp.

41. V. V. Lemanov, B. V. Sukharev, V. V. Kludzin, et al., "Acoustooptical Control of Laser Emission in Lithium Niobate Light Guides," PIS'MA ZHTF (Letters of the Journal of Theoretical Physics), Vol 2, No 12, 1976, pp 532-536.

42. V. V. Lemanov, O. V. Shakin, "Dispersion of Light on Elastic Waves in Uniaxial Crystals," FIZIKA TVERDOGO TELA (Solid State Physics), vyp. 1, No 14, 1972, pp 229-264.

43. J. Nay, FIZICHESKIY SVOYSTVA KRISTALLOV (Physical Properties of Crystals), Moscow, Mir, 1967.

44. A. I. Naydenov, TRANSFORMATSIYA SPEKTRA NANOSEKUNDNYKH IMPUL'SOV (Transformation of a Nanosecond Pulse Spectrum), Moscow, Sovetskoye radio, 1973, 180 pp.

45. A. Papulis, TEORIYA SISTEM I PREOBRAZOVANIY V OPTIKE (Theory of Systems and Conversions in Optics), Moscow, Mir, 1971, 495 pp.

46. V. P. Pikarnikov, "High-Frequency Ultrasonic Converters and Their Application in Optoacoustic Devices," Author's Review of Candidate's Dissertation, LIAP, 1973.

47. B. P. Razzhivin, D. V. Tigin, "Transmission Coefficient and Pulse Response of a Simple Optical Filter," TRUDY LIAP (Works of the LIAP Institite), No 75, 1975, pp 161-165.

48. S. M. Rytov, "Light Diffraction on Ultrasonic Waves," IZV. AN SSSR. SER. FIZICH. (News of the USSR Academy of Sciences. Physics Series), No 2, 1937, 222 pp.

49. J. Reley, VOLNOVAYA TEORIYA SVETA (Light Wave Theory), Moscow, Gostekhizdat, 1940, p 208.

50. A. V. Solodov, F. S. Petrov, LINEYNYYE AVTOMATICHESKIYE SISTEMY S PEREMENNYMI PARAMETRAMI (Linear Automated Systems with Variable Parameters), Moscow, Nauka, 1971, 620 pp.

51. K. I. Tarasov, SPEKTRAL'NYYE PRIBORY (Spectral Devices), Leningrad, Mashinostroyeniye 1968, 388 pp.

52. V. I. Tverskoy, DISPERSIONNO-VREMENNYYE METODY IZMERENIY SPEKTROV RADIOSIGNALOV (Dispersion-Time Methods of Measuring Radio Signal Spectra), Moscow, Sovetskoye radio, 1974, 240 pp.

53. FIZICHESKAYA AKUSTIKA (Physical Acoustics), Edited by W. Mason, Moscow, Mir, Vol 1A, 1968, 548 pp.

54. FIZICHESKAYA AKUSTIKA (Physical Acoustics), Edited by W. Mason and R. Thurston, Moscow, Mir, Vol 7, 1974, 429 pp.

55. M. Franson, S. Slanskiy, KOGERENTNOST' V OPTIKE (Coherence in Optics), Moscow, Nauka, 1967, 80 pp.

56. A. A. Kharkevich, SPEKTRY I ANALIZ (Spectra and Analysis), Moscow, Fizmatgiz, 1962, 236 pp.

57. V. M. Chernitser, B. G. Kaduk, PREOBRAZOVATELI VREMENNOGO MASSHTABA (Time Scale Converters), Moscow, Sovetskoye radio, 1972, 144 pp.

58. S. M. Shandarov, "Study of Schaffer-Bergman Diffraction in a Lithium Niobate Crystal on Hypersonic Frequencies," FIZIKA TVERDOGO TELA (Solid State Physics), Vol 15, No 9, 1973, pp 2586-2590.

59. E. Abbe, GESAMMELTE ABHANDLUNGEN, G. Fischer, Jena, 1904.

60. A. Aliopi, L. Palmiery, "Spectrum Analysis of the Light Diffracted by an Ultrasonic Standing Wave by Means of a Holographic Method," ACUSTICO, Vol 21, No 2, 1969, pp 104-111.

61. D. L. Arenberg, "Ultrasonic Solid Delay Lines," JASA, Vol 20, No 1, 1948, pp 1-26.

62. H. Aritome, T. Ikegoni, T. Nishimura, et al., "Formation of Optical Wave Guides by Ion Implantation into Fused Quartz," PROC. 4TH CONFER. OF SOLID STATE DEVICES, Tokyo, 1972, pp 136-144.

63. C. Atzeni, L. Pantani, "Optical Signal Processing through Dualchannel Ultrasonic Light Modulator," PROC. IEEE, Vol 58, No 3, 1970, pp 501-502.

64. M. Arm, L. Lambert, I. Weisman, "Optical Correlation Techniques for Radar Plus Compression," PROC. IEEE, Vol 52, 1964, p 842.

65. C. Atzeni, "Optical Signal Processing by Filtering Fresnel Images of Acoustic Light Modulators," APPL. OPT., Vol 11, No 4, 1972, pp 863-872.

66. C. Atzeni, L. Pantani, "A Simplified Optical Correlator for Radar Signal Processing," PROC. IEEE, Vol 57, No 3, 1969, pp 344-346

67. H. E. Bommel, K. Dransfeld, "Excitation and Attenuation of Hypersonic Waves in Quartz," PHYS. REV., Vol 117, No 3, 1960, p 1245.

68. H. Born, E. Wold, PRINCIPLES OF OPTICS, New York, Pergamon Press, 1959.

69. C. F. Brockelsby, I. S. Palfreeman, R. W. Gibson, ULTRASONIC DELAY LINES, London, 1963.

70. H. A. Brouneus, W. H. Jenkins, "Photoelastic Ultrasonic Delay Line," PROC. OF THE NAT. ELECTRONICS CONFERENCE, Vol 16, 1960, p 835.

71. H. A. Brouneus, W. H. Jenkins, "Continuously Variable Glass Delay Lines," ELECTRONICS, Vol 34, No 2, 1961.

72. W. I. Caputi, "Stretch: a Time-Transformation Technique," IEEE TRANS., AES-7, No 2, 1971, pp 269-273.

73. H. R. Carleton, W. Maloney, G. Meltz, "Collinear Heterodyning in Optical Processors," PROC. IEEE, Vol 57, No 5, 1969, pp 769-775.

74. M. G. Cohen, E. I. Gordon, "Acoustic Beam Probing using Optical Techniques," BELL SYST. TECHN. JOURN., Vol 44, No 4, 1965, pp 693-721.

75. J. H. Collins, E. G. Lean, H. J. Show, "Pulse Compressing by Bragg Diffraction of Light with Microwave Sound," APPL. PHYS. LETT., Vol 11, No 7, 1967, pp 240-242.

76. G. A. Coquin, D. A. Pinnow, A. W. Warner, "Physical Properties of Lead Molybdate Relevant to Acoustooptic Device Applications," JOURN. APPL. PHYS. Vol 42, No 6, 1971, pp 2162-2168.

77. L. I. Cutrona, E. N. Leith, C. I. Palermo, et al., "Optical Data Processing and Filtering Systems," IRE TRANS. OF INFORMATION THEORY, Vol 6, 1960, pp 386-400.

78. R. W. Dixon, M. G. Cohen, "New Technique for Measuring Photoelastic Tensor and Its Applications to Lithium Niobate," APPL. PHYS. LETT., Vol 8, 1966, p 205.

79. E. B. Felstead, "A Simple Real Time Incoherent Optical Correlator," IEEE TRANS. ON AEROSPACE AND ELECTRONIC SYSTEMS, Vol AES-3, No 6, 1967, pp 907-914.

80. I. S. Gerig, H. Montague, "A Simple Optical Filter for Chirp Radar," PROC. IEEE, Vol 52, No 12, 1964, p 1753.

81. M. Gottlieb, J. J. Conroy, T. Forster, "Optoacoustic Processing of Large Time-Band Width Signals," APPL. OPT., Vol 11, No 5, 1972, pp 1068-1077.

82. M. Gottlieb, J. J. Conroy, "Design and Construction of an Optoacoustic Signal," APPL. OPT., Vol 12, No 8, 1973, pp 1922-1927.

83. H. L. Groginsky, I. D. Young, "A New Technique for Simultaneous Radar Observation of Multiple Targets within a Broad Surveillance Region," IEEE, INT. CONV. REC., Vol 11, Pt 8, 1963, pp 82-91.

84. S. S. Harris, S. T. K. Nich, R. S. Feigelson, "$CaMoO_4$ Electronically Tunable Optical Filter," APPL. PHYS. LETT., Vol 17, No 5, 1970, pp 223-225.

85. S. E. Harris, R. W. Wallace, "Acoustooptic Tunable Filter," JASA, Vol 59, No 6, 1969, pp 744-747.

86. H. C. Huang, I. D. Knox, R. Wargo, et al., "Fabrication of Submicrowave Acoustic (Bulk) Delay Lines," APPL. PHYS. LETT., Vol 24, No 3, 1974, pp 109-111.

87. B. I. Hunsinger, "Spatial Modulation of Light using Surface Waves in an Interferometer," APPL. PHYS. LETT., Vol 16, No 7, 1970, pp 272-273.

88. "Improved Radar Performance Offered by Lockheed Optical Correlator," SOLID STATE DESIGN COMMUNICATIONS AND EQUIPMENT, Vol 6, No 8, 1965, p 10.

89. N. Izzo, "Optical Correlation Technique using a Variable Reference Function," PROC. IEEE, Vol 53, No 11, 1965, pp 1740-1741.

90. I. P. Kaminov, "Optical Waveguide Modulators," IEEE TRANS, Vol MTT-23, No 1, 1975, pp 57-70.

91. H. King, W. R. Bennett, L. B. Lambert, et al., "Real Time Electrooptical Signal Processors with Coherent Detection," APPL. OPT., Vol 6, No 8, 1967, pp 1367-1375.

92. D. G. King, T. I. Woods, "Pulse Compression by Optical Correlation Techniques," THE MARCONI REVIEW, Vol 31, No 171, 1968, pp 209-239.

93. W. R. Klein, B. D. Cook, "Unified Approach to Ultrasonic Light Diffraction," IEEE TRANS, Vol SU-14, No 3, 1967, pp 123-134.

94. M. Kondo, I. Ohta, F. Saito, et al., "Acoustooptic Diffraction by an Acoustic Surface Wave in an Ion Exchanged Waveguide," ELECTRON. LETT., Vol 10, No 24, 1974, pp 518-519.

95. L. Kuhn, M. L. Dakes, P. F. Heidrich, et al., "Deflection of an Optical Guided Wave by a Surface Acoustic Wave," APPL. PHYS. LETT., Vol 17, No 6, 1970, pp 265-267.

96. L. B. Lambert, "Wide Band Instantaneous Spectrum Analyzers Employing Delay Line Light Modulators," IRE INT. CONV. REC., pt 6, 1962, pp 69-78.

97. L. Lambert, M. Arm, A. Aimette, "Electrooptical Signal Processors for Phased Array Antennas," OPTICAL AND ELECTROOPTICAL INFORMATION PROCESSING, M. I. T. Press, 1966.

98. V. Lattore, "Protective Digital Transmissions with Optical Matched Filters," ELECTRONICS, Vol 38, No 10, 1965, p 76.

99. E. G. H. Lean, C. G. Powell, "Optical Probing of Surface Acoustic Waves," PROC. IEEE, Vol 52, No 12, 1970, pp 1939-1947.

100. I. K. Lee, S. Wang, "Tantalum Oxide Light Guide on Lithium Tantalate," APPL. PHYS. LETT., Vol 25, No 3, 1974, pp 164-166.

101. W. Liben, L. A. Twigg, "A Variable Ultrasonic Electrooptical Delay Line and a New Ultraoptical Effect in Fused Quartz," J. APPL. PHYS, Vol 3, No 1, 1962, p 249.

102. I. M. Lin, R. E. Cireen, "Optical Probing of Ultrasonic Diffraction in Single Crystal Sodium Chloride," JASA, Vol 53, No 2, 1973, pp 468-478.

103. W. E. Maher, G. Roome, "Large Time band Width Product Acoustooptic Correlator and Its use in a Cascade Design Matched Filter," APPL. OPT., Vol 12, No 6, 1974, pp 1342-1344.

104. D. I. McLean, L. B. Lambert, M. Arm, et al., "An Electrooptical Processor for the Radioheliograph," PROC, IEEE AUSTRALIA, Vol 28, No 9, 1967, pp 375-380.

105. D. H. McMahan, "Wideband Pulse Compression via Brillouin Scattering in Bragg Limit," PROC. IEEE, Vol 55, No 9, 1967, pp 1602-1612.

106. G. Meltz, W. Maloney, "Optical Correlation of Fresnel Images," APPL. OPT., Vol 7, No 10, 1968, pp 2091-2099.

107. H. Muller, "Theory of Photoelastic Effect of Cubic Crystals," PHYS. REV. Vol 47, 1935, pp 447-457.

108. Y. Nakazato, Y. Miura, T. Namekava, et al., "A Correlator using the Diffraction of Light by Ultrasonic Waves," J. ACOUST. SOC. JAPAN, Vol 24, No 2, 1968, pp 95-103.

109. J. Noda, T. Saku, N. Uchida, "Fabrication of Optical Waveguiding Layer in $LiTaO_3$ by Cu Diffusion," APPL. PHYS. LETT., Vol 25, No 5, 1974, pp 308-310.

110. T. Noguchi, H. Fukukita, A. Fukuma, "Simple Nitrasonic Welding Method for Bonding Thickness Mode Transducers," IEEE TRANS, Vol SU-21, No 1, 1974, pp 55-56.

111. I. S. Palfreeman, "Ein Optoakustischer Kreuz-Korrelator zur Erkennung von Radarsignalen," PHYLIPS TECHNISCHE RUNDSCHAU, No 8-10, S, 1967, pp 318-327.

112. D. A. Pinnow, "Guide Lines for the Selection of Acoustooptic Materials," IEEE, Vol QE-6, No 4, 1970, pp 223-238.

113. C. F. Quate, C. D. Wilkinson, D. R. Winslow, "Intersection of Light Microwave Sound," PROC. IEEE, Vol 53, 1965, pp 1604-1623.

114. C. V. Raman, N. S. N. Nath, "Diffraction of Light by High Frequency Sound Waves," PROC. INDIAN ACAD. SC., Vol A2, 1935, pp 406-413; Vol A3, 1936, pp 75-119.

115. E. Salzman, D. Weismann, "Optical Detection of Rayleigh Waves," J. APPL. PHYS. Vol 40, 1969, pp 3408-3400.

116. I. Sato, M. Ueda, "On Electrooptical Circuit Simulator," BULL. OF THE TOKYO INSTITUTE OF TECHNOLOGY, No 92, 1969, pp 43-50.

117. M. B. Schulz, M. G. Holland, L. Davis, "Optical Pulse Compression Using Bragg Scattering by Ultrasonic Waves," APPL. PHYS. LETT., Vol 11, No 7, 1967, pp 237-240.

118. T. H. Slaymaker, "Real Time Debye Sears Effect Spectrum Analyzer for Audio Frequencies," JASA, Vol 44, No 4, 1968, pp 1140-1142.

119. L. Slobodin, "Optical Correlation Technique," PROC. IEEE, Vol 51, 1963, p 1782.

120. L. Slobodin, "Optical Correlation of Electronic Pulses," US. Patent, No 3582635, 1961, Cl. 235-181.

121. H. Stark, "Electrooptical Processing for Radioastronomy," PROC. IEEE, Vol 60, No 8, 1972, pp 1009-1010.

122. N. Takai, "Spectrum Analyzer for Area Charts using Electrooptical Signal Processing," OPTOELECTRONICS, Vol 4, No 1, 1972, pp 31-42.

123. P. Tournois, "Analyse spectrale et filtrage adapte des signaux basse frequence en temps reel aprescompression de temps," L'ONDE ELECTRIQUE, Vol 49, No 9, 1969, pp 952-959.

124. N. Uchida, N. Nilzeki, "Acoustooptic Deflection Materials and Techniques" PROC. IEEE, Vol 61, No 8, 1973, pp 1073-1092.

125. N. Uchida, S. Sato, "Acoustooptic Tunable Filter Using TeO_2" PROC. IEEE, Vol 62, No 9, 1974, pp 1279-1280.

126. M. P. Wenkoff, M. Katchky, "An Improved Read in Technique for Optical Delay Line Correlators," APPL. OPT., Vol 9, No 1, 1970, pp 135-147.

127. D. A. Wille, M. C. Hamilton, "Acoustooptic Deflection in Ta_2O_2 Wave Guides," APPL. PHYS. LETT., Vol 24, No 4, 1974, pp 155-160.

END

10845
CSO: 8144/1398